

TR/BR-16/99-2000

# **MODELLING OF SEAWATER INTRUSION**



**NATIONAL INSTITUTE OF HYDROLOGY  
JALVIGYAN BHAWAN  
ROORKEE - 247 667 (UTTARANCHAL)**

**1999-2000**

## Preface

Coastal aquifers form a vital source of freshwater along the lengthy Indian coastline, and are increasingly being tapped to meet the water-supply needs. However, indiscriminate groundwater development of coastal regions may result in gradual encroachment of seawater, which deteriorates the quality of groundwater and may ultimately render it unfit for human use. There have been instances, where large-scale seawater intrusion has forced the farmers to desert their once thriving farmlands. On the eastern coast of India, the seawater intrusion problem is further compounded because the growing demand for seafood has lead many a farmer to take to aquaculture as a more profitable source of income. The water quality in these aquaculture tanks is usually saline, which slowly infiltrates and reaches the water table. Besides this, the cyclonic storms are a recurring feature in this area, as a result of which the affected coastal belt gets submerged underneath a blanket of salinewater. Before any further groundwater development of this region is carried out it is essential to gain an understanding of the changes in the dynamics of a coastal aquifer system when it is subject to varying hydrologic conditions. In the present study, the seawater intrusion phenomenon has been numerically simulated and the effect of salinewater recharge on an underlying coastal aquifer has been analysed.

This report entitled 'Modelling of Seawater Intrusion' is a part of the research activities of 'Groundwater Assessment Division' of the Institute. The study has been carried out by Dr. Anupma Sharma, Scientist 'B'.



**(K.S. Ramasastri)**

Director

# CONTENTS

LIST OF FIGURES.....	iv
LIST OF TABLES.....	iv
ABSTRACT.....	v
<b>1.0 INTRODUCTION.....</b>	<b>1</b>
<b>2.0 LITERATURE REVIEW.....</b>	<b>3</b>
2.1 General .....	3
2.2 Modelling Approaches .....	3
2.3 Sharp Interface Models .....	4
2.4 Miscible Transport Models.....	8
2.5 Comparison of the Sharp Interface and Miscible Transport Modelling Approaches .....	16
<b>3.0 MODEL DEVELOPMENT.....</b>	<b>17</b>
3.1 Problem Definition .....	17
3.2 Governing Equations.....	18
3.3 Solution Domain.....	20
3.4 Coordinate System.....	21
3.5 Initial and Boundary Conditions for Saltwater Transport.....	21
3.6 Initial and Boundary Conditions for Fluid Flow.....	23
3.7 The Solution Strategy .....	24
<b>4.0 MODEL VALIDATION.....</b>	<b>25</b>
4.1 Henry's Problem.....	26
4.1.1 Model Operation .....	26
4.1.2 Results and Discussion.....	28
<b>5.0 MODEL APPLICATION.....</b>	<b>30</b>
5.1 Hypothetical Problem .....	31
5.1.1 Model Operation .....	32
5.1.2 Results and Discussion.....	33
5.2 Simulation of Hypothetical Scenarios of Vertical Salinewater Recharge.....	34
5.2.1 Model Operation - Stage I .....	34
5.2.1.1 Results and Discussion .....	36
5.2.2 Model Operation - Stage II.....	43
5.2.2.1 Results and Discussion .....	43
5.3 Effect of Anisotropy on Salinewater Recharge.....	45

<b>6.0 CONCLUSIONS.....</b>	<b>49</b>
<b>REFERENCES.....</b>	<b>50</b>
<b>APPENDIX-I .....</b>	<b>54</b>
<b>APPENDIX-II.....</b>	<b>57</b>

## LIST OF FIGURES

Fig.1 Solution domain.....	20	
Fig.2 Concentration distribution at steady state (Henry's Problem).....	29	
Fig.3 Comparison of computed 0.5 isochlor with Henry's semi-analytical solution and SUTRA numerical solution .....	29	
Fig. 4 Definition sketch of hypothetical problem.....	31	
Fig. 5 Concentration distribution at steady state (Hypothetical Problem).....	33	
Fig. 6 Concentration distribution at steady state with no vertical recharge (Initial Condition for Stage I) .....	34	
Fig. 7 Steady state velocity distribution with no vertical recharge (Initial Condition for Stage I) .....	35	
Fig. 8 Concentration distribution at steady state, Stage I - Case I .....	37	37
Fig. 9 Concentration distribution at steady state, Stage I - Case II .....	38	
Fig. 10 Concentration distribution at steady state, Stage I - Case III.....	39	
Fig. 11 Steady state velocity field, Stage I - Case III for $c^* = 1$ .....	40	
Fig. 12 Concentration distribution with recharge $c^* = 0.5$ , Stage I - Case III (Transient state at early times).....	41	
Fig. 13 Concentration distribution with recharge $c^* = 0.5$ , Stage I - Case III (Transient state at later times).....	42	
Fig. 14 Concentration distribution after 90 days, Stage II - Case I .....	44	
Fig. 15 Concentration distribution after 90 days, Stage II - Case II .....	44	
Fig. 16 Effect of anisotropy on salinewater recharge: Concentration distribution at steady state with recharge $c^* = 0.5$ over 75% length of domain.....	46	
Fig.17(a) Steady state velocity field with recharge $c^* = 0.5$ over 75% length of domain, anisotropy = 2 .....	47	
Fig.17(b) Steady state velocity field with recharge $c^* = 0.5$ over 75% length of domain, anisotropy = 50 .....	48	

## LIST OF TABLES

Table 1 Parameter Values for Henry's Problem.....	26
---	----

## Abstract

Coastal aquifers that are in hydraulic continuity with the sea are vulnerable to seawater intrusion. Besides the lateral intrusion of seawater, the coastal aquifer may also be subject to a vertical recharge of salinewater due to submergence of land under salinewater during cyclonic storms and infiltration of salinewater from aquaculture tanks. This is a familiar scenario along the low-lying eastern coast of India. Under such conditions, the dynamic equilibrium existing between freshwater and seawater in a coastal aquifer may get disturbed. For a sustainable development of these coastal aquifers, it is thus essential to know the response of the freshwater-saltwater interface for a given hydrologic condition.

In this study, a two-dimensional numerical model in the vertical plane for simulating miscible transport of saltwater in a coastal aquifer has been developed. In order to simulate the variable density flow, the governing partial differential equations of flow and solute transport have been written in terms of pressure and concentration, respectively. The Iterative Alternating Direction Implicit (IADI) scheme of finite differences has been used to solve these non-linear equations. Density coupling of these equations is accounted for and handled using a Picard sequential solution algorithm with provision for automatic reduction of time step values when the stipulated number of iterations is exceeded. The model has been validated using the semi-analytical solution of the benchmark Henry's Problem for saltwater intrusion in a coastal aquifer as well as the SUTRA numerical solution for this test problem. Different hypothetical scenarios have been simulated using the model, to evaluate the short-term and long-term effect of vertical salinewater recharge on the freshwater-seawater mixing zone.

## 1.0 INTRODUCTION

All over the world industrial, urban and tourist complexes occupy much of the coastal margin of most of the developed and developing countries. The low-lying coastal areas, especially the large deltaic regions, are important areas of agricultural production. The Indian peninsula has a long coastline of about 7000 km. Water resources in these coastal areas have a special meaning since any developmental activity will largely depend upon the availability of freshwater to meet the industrial, agricultural and domestic requirements. As the surface water in coastal areas is generally saline and under tidal influence, groundwater from the coastal aquifers meets the major bulk of such requirements.

However, coastal aquifers which are in hydraulic continuity with saline water bodies are subject to intrusion of saline water, the extent of which depends upon climatic conditions, the hydrogeology of area, and the manner and degree of development of these aquifers. Once an aquifer is completely intruded by seawater due to extensive lowering of the water table, it becomes extremely difficult to reclaim the much - needed freshwater. In India, most of the states lying along the coast are facing the above threatening scenario. Besides this, the freshwater aquifers on the low-lying eastern coast of India are vulnerable to contamination from other sources as well, e.g., infiltration of salinewater from aquaculture tanks and repeated flooding of the coastal area with salinewater during cyclonic storms. Under these conditions, the coastal aquifer is subject to both lateral intrusion of saltwater from the sea as well as a vertical recharge of salinewater.

For a sustainable development of the coastal regions, it is thus essential to have a prior knowledge of the immediate and long term transient behaviour of the coastal aquifer system in response to given hydrologic conditions. Mathematical modelling of the coastal aquifer system is an indispensable tool in such cases.

Seawater intrusion occurs mainly on account of seawater transport by advection and hydrodynamic dispersion. Advection is the transport of solute by the bulk motion of the flowing groundwater. Further spreading of the solute from its expected advective path

occurs because of hydrodynamic dispersion, which comprises molecular diffusion and mechanical dispersion (i.e., mechanical mixing during fluid advection).

In coastal aquifers, due to hydrodynamic dispersion, the zone of contact between freshwater and seawater takes the form of a transition zone (henceforth, also referred to as the disperse interface) across which the salt concentration and hence density of saltwater varies from that of freshwater to that of seawater. In this zone, the diluted seawater rises and moves seaward causing saltwater from the sea to flow towards the transition zone. This induces a cyclic flow of seawater from the floor of the sea to the transition zone and finally back to the sea. As a result of this circulation of seawater, the toe of the disperse interface is displaced towards the seaward side (Cooper et al., 1964).

Numerical models to simulate seawater intrusion either account only for advection (sharp interface models) or for both advection and hydrodynamic dispersion (miscible transport models). However, from the discussion in the preceding paragraph it is clear that in order to obtain a better estimate of the real nature and position of the interface between freshwater and seawater, it is vital to account for the effects of hydrodynamic dispersion. In addition, through such a miscible transport model, the amount of seawater present in the water arriving at supply wells can also be estimated with adequate resolution. The usefulness of this can be gauged from the fact that water of potable quality contains less than about 1% seawater. On the other hand, a sharp interface model can discriminate only between freshwater and seawater.

In the present study, a two-dimensional numerical model in vertical plane has been developed to simulate the intrusion of seawater in a coastal aquifer. The model is based upon the more realistic disperse interface approach wherein freshwater and saltwater are taken as miscible fluids. The model has been validated using the benchmark Henry's Problem. The effect of vertical salinewater recharge on a coastal aquifer has been analysed by simulating possible hypothetical scenarios.



## **2.0 LITERATURE REVIEW**

### **2.1 General**

The earliest attempts to define the position of freshwater-saltwater interface were made at the end of 19<sup>th</sup> century, which were based on the principle of hydrostatic equilibrium. At the beginning of the second half of 20<sup>th</sup> century, a large number of field investigations were conducted which gave a fresh insight into the dynamics of coastal aquifers.

In recent years, a phenomenal rise has been witnessed worldwide in the general awareness and interest in the problem of seawater intrusion in coastal aquifers. To combat the problem, it is essential to first understand the general characteristics and behaviour of a coastal aquifer system subject to varying hydrologic conditions. A significant portion of groundwater literature is devoted exclusively for this purpose. The following sections contain a brief review of some of the more well-known and widely used mathematical models, analytical as well as numerical, to simulate the behaviour of coastal aquifers.

### **2.2 Modelling Approaches**

The mathematical analysis of the seawater intrusion problem may involve several simplifying assumptions. One such assumption, which classifies the models developed so far into two distinct groups, is regarding the presence of transition zone. If the width of this zone is small relative to the thickness of the aquifer then it is assumed, for the purpose of analysis, that the seawater and freshwater are immiscible fluids separated by a sharp interface instead of the disperse interface. In view of the above, the mathematical models reviewed here are broadly classified as follows:

- Sharp Interface Models
- Miscible Transport Models

The review of mathematical models is restricted to that category of models, which analyse the intrusion problem at regional scale.

### 2.3 Sharp Interface Models

The sharp interface models require simultaneous solution of freshwater and saltwater flow equations coupled by the boundary condition that specific discharge and pressure must be equal on either side of the sharp interface (i.e., the freshwater and saltwater regions). The equation of flow in the freshwater region is (Bear, 1979)

$$\frac{\partial}{\partial x} \left( K_{xf} \frac{\partial h_f}{\partial x} \right) + \frac{\partial}{\partial y} \left( K_{yf} \frac{\partial h_f}{\partial y} \right) + \frac{\partial}{\partial z} \left( K_{zf} \frac{\partial h_f}{\partial z} \right) + Q_f = S_{yf} \frac{\partial h_f}{\partial t} \quad (1a)$$

and for saltwater region it is

$$\frac{\partial}{\partial x} \left( K_{xs} \frac{\partial h_s}{\partial x} \right) + \frac{\partial}{\partial y} \left( K_{ys} \frac{\partial h_s}{\partial y} \right) + \frac{\partial}{\partial z} \left( K_{zs} \frac{\partial h_s}{\partial z} \right) + Q_s = S_{ys} \frac{\partial h_s}{\partial t} \quad (1b)$$

where  $x$  and  $y$  are the coordinates in the horizontal plane;  $z$  is the coordinate along the vertical direction;  $t$  is time;  $h$  is the hydraulic head;  $K_x$ ,  $K_y$ , and  $K_z$  are hydraulic conductivities in  $x$ -,  $y$ - and  $z$ -directions, respectively;  $S_s$  is the specific storage;  $Q$  is the source/sink term (-ve for sink); and subscripts  $f$  and  $s$  refer to freshwater and saltwater, respectively.

Sometimes, instead of the freshwater and saltwater heads, the freshwater head and the position of the interface are taken as independent variables (e.g. Eem, 1992). However, due to mathematical complexity of the problem, several types of approximations have been employed by various researchers to obtain the analytical and numerical solutions.

To reduce the dimensionality of the problem, researchers often simulate intrusion in 2-D horizontal plane by invoking Dupuit assumptions (also known as the hydraulic approach). In this case, the representative equations are obtained by integrating the flow equations (Eqs. (1a) and (1b)) for each fluid over the vertical dimension. The solution of

these equations, subject to appropriate boundary conditions, provides the values of freshwater and saltwater hydraulic heads. The position and shape of the interface is then obtained using Eq. (3) described later in this section.

Instead of the two-fluid approach mentioned above, some of the sharp interface models incorporate, as an additional simplifying assumption, the Ghyben-Herzberg approximation. This transforms the two-fluid problem into a one-fluid problem. The one-fluid approach makes it possible to solve for freshwater flow only. Here, it is assumed that the saltwater flow region instantaneously adjusts to changes in the freshwater flow region. Essaid (1986) observed that the one-fluid approach neglects the influence of saltwater flow on the freshwater head distribution. Therefore, this approach is suitable for reproducing the long term responses only. The two-fluid approach is more appropriate for investigating short term responses.

### Analytical Solutions

The *Ghyben-Herzberg principle* proposed by Badon-Ghyben (1889) and Herzberg (1901) was the first quantitative analysis of the interface position and is still widely used in field to arrive at a quick estimate of the interface position. It relates the freshwater head above sea level ( $\Phi_f$ ) to the depth of the interface below sea level ( $\zeta_s$ ) for a system in static equilibrium, i.e., steady horizontal freshwater flow and stationary saltwater. At the interface, the pressure due to the overlying column of freshwater must be equivalent to that due to the column of saltwater, therefore the following relation holds:

$$\begin{aligned} \zeta_s \gamma_s &= (\zeta_s + \Phi_f) \gamma_f \\ \text{or} \quad \zeta_s &= \delta \Phi_f \end{aligned} \tag{2}$$

where  $\delta = \gamma_f / (\gamma_s - \gamma_f)$ . For common values of freshwater and saltwater densities ( $1.0 \text{ gm/cm}^3$  and  $1.025 \text{ gm/cm}^3$ , respectively) the value of  $\delta$  is 40. This implies, the depth to the interface below sea level is forty times the freshwater head. In groundwater literature, the assumption of stationary saltwater is commonly known as the Ghyben-Herzberg approximation.

The erroneous result inherent in Eq. (2) is that the thickness of freshwater zone is represented as zero at the shore where the elevation of water table is zero. This is because the Ghyben-Herzberg principle relates the head at the water table to the position of interface.

Hubbert (1940) improved upon the Ghyben-Herzberg principle by formulating the following equation which relates the freshwater head ( $h_f$ ) and saltwater head ( $h_s$ ) at a point on the interface to its elevation ( $Z_i$ ):

$$Z_i = \frac{\gamma_s}{\gamma_s - \gamma_f} h_s - \frac{\gamma_f}{\gamma_s - \gamma_f} h_f \quad (3)$$

where  $\gamma_s$  is the specific weight of saltwater and  $\gamma_f$  is the specific weight of freshwater, respectively.

Glover (1959) developed the following expression to describe the position of the interface accounting for the movement and discharge of freshwater from a coastal aquifer, under steady flow conditions:

$$Z - \frac{2Q}{\Delta\gamma K} x - \frac{Q^2}{(\Delta\gamma)^2 K^2} = 0 \quad (4)$$

where  $Q$  is the freshwater flow per unit length of shore;  $K$  is the hydraulic conductivity of the medium;  $x$  is the distance from the shore;  $Z$  is the depth from mean sea level;  $\Delta\gamma = (\rho_s - \rho_f)/\rho_f$ ;  $\rho_f$  is the density of freshwater; and  $\rho_s$  is the density of seawater. The above formula was derived using Ghyben-Herzberg approximation.

### Numerical Solutions

Essaid (1990) presented a quasi-3-D model (SHARP) to simulate the transient interface in a layered coastal aquifer. The freshwater and saltwater flow equations for each aquifer were formulated using the hydraulic approach. Leakage between aquifers was

calculated by applying Darcy's law. The governing equations were approximated and solved using the finite difference method with strongly implicit procedure. The positions of the tip and toe were tracked using linear extrapolation of the interface elevations calculated at grid points. The model was verified against an analytical solution for a linear interface, and Hele-Shaw experimental results (Bear and Dagan, 1964). Essaid used the model for an areal steady state simulation of southeastern Oahu aquifer and cross-sectional steady state simulation of Cape May layered aquifer, New Jersey. Spitz and Barringer (1992) used the SHARP model to simulate seawater encroachment in the shallow aquifer system in the peninsula of Cape May County, New Jersey. In their optimization model for the control of seawater intrusion in the Jakarta groundwater basin in Indonesia, Willis and Finney (1991) used the SHARP model to simulate the location of interface.

Mahesha (1995) developed a finite element model incorporating Dupuit assumptions to simulate the transient motion of interface as a consequence of a constant lowering of freshwater level in an unconfined coastal aquifer. The model was used to perform parametric studies on an advancing interface for hypothetical cases. From these studies it was inferred that the advancement of the interface is dependent on the rate, location and period of freshwater level variations. Mahesha (1996) derived the steady state position of interface both due to an extraction well system and in combination with an injection well system in coastal confined aquifers. A number of cases with different combinations of the number and location of the series of wells, spacings of wells and the injection-extraction rates were considered. It was found that for larger well spacings and smaller rates of injection, the injection-extraction well system was more effective in controlling seawater intrusion.

During the period 1940-1965 extensive field investigations were carried out in the Netherlands, Israel, and the United States. These contributed to a deeper understanding of freshwater-saltwater dynamics and led to a more realistic modelling of the seawater intrusion process. A number of models developed henceforth accounted for the presence of the transition zone in a coastal aquifer, which in the following review have been termed as 'miscible transport models'.

## 2.4 Miscible Transport Models

In miscible transport models, the problem of seawater intrusion is posed as that of a variable density fluid flow accounting for the effects of dispersion. The models require the simultaneous solution of the coupled groundwater flow and advective-dispersive equations. For a variable density fluid, the groundwater flow equation is (Bear, 1979)

$$\frac{\partial}{\partial x} \left( \frac{\kappa_x \gamma}{\mu} \frac{\partial p}{\partial x} \right) + \frac{\partial}{\partial y} \left( \frac{\kappa_y \gamma}{\mu} \frac{\partial p}{\partial y} \right) + \frac{\partial}{\partial z} \left[ \frac{\kappa_z \gamma}{\mu} \left( \frac{\partial p}{\partial z} + \gamma \right) \right] + W \gamma^* = S_s \frac{\partial p}{\partial t} + \phi \frac{\partial \gamma}{\partial c} \frac{\partial c}{\partial t} \quad (5)$$

where  $p$  is the fluid pressure;  $\kappa_x$ ,  $\kappa_y$ , and  $\kappa_z$  are the intrinsic permeabilities in the  $x$ -,  $y$ - and  $z$ -directions, respectively;  $\gamma$  is the specific weight of fluid;  $S_s$  is the specific storage of porous medium;  $\mu$  is the dynamic viscosity of fluid;  $\gamma^*$  is the specific weight of source or sink fluid;  $\phi$  is porosity;  $c$  is fluid concentration; and  $W$  is the source/sink volume flux per unit volume of porous medium (+ve for inflow).

The last term on the right side of Eq. (5), represents the rate of change in specific weight due to a change in concentration over time. Since the contribution of this term compared to other terms is small, it is mostly neglected.

The Darcy velocities in  $x$ ,  $y$  and  $z$  directions are given by

$$q_x = - \frac{\kappa_x}{\mu} \frac{\partial p}{\partial x} \quad (6a)$$

$$q_y = - \frac{\kappa_y}{\mu} \frac{\partial p}{\partial y} \quad (6b)$$

$$q_z = - \frac{\kappa_z}{\mu} \left( \frac{\partial p}{\partial z} + \gamma \right) \quad (6c)$$

The advective-dispersive equation describing the transport of dissolved salt (assuming no chemical reactions and no interaction with the solid matrix) is (Bear, 1979)

$$\begin{aligned} \frac{\partial}{\partial x} \left[ \phi \left( D_{xx} \frac{\partial c}{\partial x} + D_{xy} \frac{\partial c}{\partial y} + D_{xz} \frac{\partial c}{\partial z} \right) \right] + \frac{\partial}{\partial y} \left[ \phi \left( D_{yx} \frac{\partial c}{\partial x} + D_{yy} \frac{\partial c}{\partial y} + D_{yz} \frac{\partial c}{\partial z} \right) \right] \\ + \frac{\partial}{\partial z} \left[ \phi \left( D_{zx} \frac{\partial c}{\partial x} + D_{zy} \frac{\partial c}{\partial y} + D_{zz} \frac{\partial c}{\partial z} \right) \right] - q_x \frac{\partial c}{\partial x} - q_y \frac{\partial c}{\partial y} - q_z \frac{\partial c}{\partial z} \\ + W(c^* - c) = \phi \frac{\partial c}{\partial t} \end{aligned} \quad (7)$$

where  $c^*$  is the concentration of the source or sink fluid; and  $D_{xx}$ ,  $D_{xy}$ ,  $D_{xz}$  etc. are coefficients of hydrodynamic dispersion.

The coefficient of hydrodynamic dispersion is defined as the sum of the coefficient of mechanical dispersion and molecular diffusion in a porous medium. For an isotropic aquifer, the coefficients of hydrodynamic dispersion can be stated explicitly as (Bear, 1979)

$$D_{xx} = \alpha_L \frac{v_x^2}{|v|} + \alpha_T \frac{v_y^2 + v_z^2}{|v|} + D_o \quad (8a)$$

$$D_{yy} = \alpha_L \frac{v_y^2}{|v|} + \alpha_T \frac{v_x^2 + v_z^2}{|v|} + D_o \quad (8b)$$

$$D_{zz} = \alpha_L \frac{v_z^2}{|v|} + \alpha_T \frac{v_x^2 + v_y^2}{|v|} + D_o \quad (8c)$$

$$D_{yx} = D_{xy} = (\alpha_L - \alpha_T) \frac{v_x v_y}{|v|} \quad (8d)$$

$$D_{zx} = D_{xz} = (\alpha_L - \alpha_T) \frac{v_x v_z}{|v|} \quad (8e)$$

$$D_{yz} = D_{zy} = (\alpha_L - \alpha_T) \frac{v_y v_z}{|v|} \quad (8f)$$

where  $\alpha_L$  is the longitudinal dispersivity and  $\alpha_T$  is the transverse dispersivity of the porous medium;  $D_0$  is the molecular diffusion coefficient;  $v_x$ ,  $v_y$  and  $v_z$  are the components of seepage velocity; and  $|\mathbf{v}|$  is the magnitude of velocity vector.

Most seawater intrusion models that have been documented to date have been based on this conventional formulation.

The governing equations are coupled via the constitutive equation which relates the specific weight of the fluid to its concentration as follows (Frind, 1982):

$$\gamma(c) = \gamma_f \left[ 1 + c \left( \frac{\gamma_s}{\gamma_f} - 1 \right) \right] \quad (9)$$

Apart from the different formulation of the governing equations, a number of researchers, while modelling transient seawater intrusion have neglected the time derivative term in the flow equation assuming the release of water from storage to have a negligible effect on the movement of seawater. In the following review, the flow equation in these particular models is referred to as a steady state equation.

### Analytical Solutions

Henry (1960, 1964) presented a semi-analytical solution for the now classical problem of seawater intrusion in a confined coastal aquifer. The hypothetical problem, now well-known as Henry's Problem, was posed by Henry in the vertical plane. It consisted of an idealized rectangular confined aquifer in contact with a freshwater reservoir on one end and the ocean on the other. Henry assumed homogeneous isotropic conditions, a steady flow, and a constant dispersion coefficient. The problem was formulated in terms of stream function and concentration. The double Fourier-Galerkin solution for the problem was given for selected values of the following dimensionless parameters:

$$\xi = \frac{\ell}{d}; \quad a = \frac{Q\rho_f}{Kd(\rho_s - \rho_f)}; \quad b = \frac{D}{Q}$$



where  $l$  is the length of aquifer;  $d$  is the thickness of aquifer;  $Q$  is the net freshwater discharge per unit length;  $K$  is the hydraulic conductivity; and  $D$  is the dispersion coefficient. Henry gave the solution in the form of streamlines and isochlors (0.1 to 0.9) for the following values of parameters:

$$\xi = 2, \quad a = 0.263, \quad b = 0.1$$

The disperse interface curves were superposed with corresponding sharp interface curves (i.e. for  $\xi = 2, a = 0.45$ ) using the analytical solution for sharp interface developed previously by Henry in 1959. Henry's analysis demonstrated the existence of seawater circulation at the bottom of aquifer, and the reduction in the landward extent of seawater penetration due to dispersion.

### **Numerical Solutions**

Most of the numerical solutions for the miscible transport models have been obtained using the finite element method. A few solutions have also been obtained using the finite difference method. However, the solution of the intrusion problem, which involves the simultaneous solution of the coupled flow and transport equations, is numerically difficult. The difficulty lies in the solution of the transport equation which comprises both the advective and dispersive components of transport. The advective component of transport equation dominates for most of the field problems. Solution of such an equation by conventional techniques viz., finite differences or finite elements is susceptible to numerical dispersion (Pinder and Gray, 1977). Numerical dispersion is a truncation error which crops up while solving the transport equation if the term proportional to the second order is neglected while approximating the first order derivatives. Procedures designed to curb numerical dispersion may require impractical small grid spacings and time steps, or may result in artificial oscillations. Oscillations manifest themselves either as concentration values higher than the maximum value, or negative concentration values. A more attractive strategy to overcome some of these difficulties is to apply the moving particle methods. These methods employ a set of moving particles for the simulation of advection. The

simulation of dispersion and other terms is carried out over a fixed mesh using finite differences or finite elements. Over the years, a variety of moving particle methods have been proposed and implemented by researchers to obtain a solution of the transport equation. Seawater intrusion models, using the moving particle methods, are largely based on the method of characteristics (MOC) proposed by Garder et al. in 1964. In literature, the method is also referred to as the particle in cell (PIC) method. Several variant forms of MOC exist in literature, which have been used to model seawater intrusion (e.g., Galeati et al., 1992; Zheng, 1993; Sharma, 1996).

However, the following brief review of miscible transport models to simulate seawater intrusion pertains only to the models based on finite differences and finite elements.

### ***Finite Difference Method***

Intercomp (1976) developed a 3-D finite difference transient model for the U.S. Geological Survey to evaluate the effects of liquid waste disposal in aquifers. The governing equations, written in terms of pressure and concentration, were solved using the finite difference method with either upstream weighting or central weighting. Testing of the model included simulation of Henry's Problem. However, the model could not attain steady state because of lengthy computations. Mercer et al. (1986) used the revised version (Intera, 1979) of the above code to simulate seawater intrusion in Volusia County, Florida. To reduce the complexities involved with 3-D simulation of a large area only 1-D flow was considered initially. As understanding of the flow system improved, solute transport and additional components of dimensionality were added until the 3-D simulation was obtained. The well known heat and transport simulator, HST3D, developed by Kipp (1987; 1997) is a descendent of the codes developed by Intercomp and Intera.

Gupta and Sivanathan (1988) described a quasi-3-D model for simulating areal transport in a two-layered aquifer system. The flow in the aquitard was considered to be vertical. The flow and transport equations, with freshwater head and concentration as the

primary dependent variables, were solved using an implicit finite difference scheme. On comparing the numerical solution with the analytical 1-D solution given by Ogata and Banks (1961), it was found that the numerical solution displayed considerable numerical dispersion for grid Peclet number exceeding one. On applying the model to a hypothetical field situation, it was found that the effect of concentration change on viscosity was not significant for source concentration in the range 25 to 30 gram/lit. A sloping aquifer bed produced appreciable effect on concentration distribution, as the flow velocity became significantly concentration dependent. They also analysed the effect of vertical leakage, in the two-layered aquifer system, on concentration distribution.

### ***Finite Element Method***

Rouve and Stoessinger (1980) used a steady flow equation with pressure as the dependent variable to formulate a Galerkin finite element model in the vertical plane with linear triangular elements. The model was applied to study the seawater movement in the Madras aquifer, India. It was shown that a small reduction in the hydraulic gradient exerted a strong influence on seawater encroachment. This highlighted the importance of controlled pumpage.

Putting emphasis on the numerical efficiency of the model, Frind (1982a) expressed the flow equation in terms of freshwater head. The model was developed in the vertical plane using the Galerkin finite element scheme and linear elements which produced a discontinuous velocity field. Using a mixed boundary condition on the seawater side of problem domain, Frind verified his numerical solution against Henry's semi-analytical solution and also compared his solution with previous numerical simulations of Henry's Problem. He also showed that the discontinuous velocity solution approached continuous velocity solution as the grid became finer. Use of the velocity-dependent dispersion coefficient was shown to produce a sharper toe. Frind (1982b) applied the above model to a confined coastal aquifer overlain by a leaky aquitard. He assumed vertical flow in the aquitard and leakage flux proportional to the head drop across it. The results indicated that the aquitard exerted a controlling influence on the dynamics of the entire system.

Huyakorn et al. (1987) developed a 3-D model to simulate seawater intrusion in single as well as multi-layered coastal aquifer systems. They adopted hydraulic head and concentration as the dependent variables in the governing equations. The model was developed using a Galerkin finite element scheme with rectangular and triangular prism elements. The vertical slicing approach was used for spatial discretization. The flow and transport in aquitards was approximated as one-dimensional. The verification and utility of the model was demonstrated by applying it to four test problems including the steady state and transient cases of Henry's Problem. The above model was enhanced by Huyakorn and Panday in 1990 to alleviate the numerical difficulties faced with a 3-D simulation, and handle situations wherein groundwater flow is significantly influenced by variations in solute concentration. The enhanced model (DSTRAM) was benchmarked using test problems discussed by Huyakorn et al. (1987). Panday et al. (1993) used the model to examine the Geneva freshwater lens, Florida. Transient simulations of various pumping scenarios were performed and it was concluded that distributed withdrawals would be more effective in managing the freshwater lens than localized withdrawals.

In an attempt to model a narrow transition zone in a coastal aquifer, Voss and Souza (1987) developed a 2-D numerical model (SUTRA) in the vertical plane for the US Geological Survey. The governing equations were written in terms of pressure and concentration. The model was developed using a weighted residual numerical method combining Galerkin finite elements with integrated finite differences. The model was verified against two test problems including Henry's Problem and was further applied to simulate the narrow transition zone in the layered basalt aquifer of southern Oahu, Hawaii (Souza and Voss, 1987). To successfully simulate a narrow transition zone, they pointed out the importance of a consistent velocity approximation. They also stressed on the need of an adequately fine spatial discretization for accurate representation of the effects of low dispersivities. Bush (1988) used the SUTRA model to simulate the effects of groundwater development in the Floridian aquifer system, Hilton Head Island, South Carolina. Reilly (1990) used the SUTRA model to examine groundwater flow in layered coastal aquifers, by considering a hypothetical system. On the basis of numerical experiments, he concluded that

for the best simulation of dispersion in layered aquifer systems either a flow-direction dependent dispersion formulation is required or the dispersivities must change spatially to reflect the tight thin confining unit. Smith (1994) applied the SUTRA model to simulate the saltwater movement in the Upper Floridian aquifer beneath Port Royal Sound, South Carolina.

Inouchi et al. (1990) analysed the problem of seawater intrusion in confined coastal aquifers under the influence of tides using a sharp interface analytical model and a miscible transport numerical model in the vertical plane. The sharp interface model was based on Ghyben-Herzberg approximation and Dupuit assumptions. It gave approximate expressions for the variation of the groundwater level and saltwater interface in response to variations of the sea level in the form of simple harmonic oscillations. The miscible transport model used Galerkin finite element method w.r.t. space coordinate and finite difference method w.r.t. time coordinate. The model produced spatial and temporal distributions of pressure and concentration. Both the models were applied to the confined coastal aquifer in the estuary of Naka river in Japan. From the analysis based on the miscible transport model, it was found that the seawater intruded furthest inland when the sea level reached the mean sea level in the ebb stage and at that time the transition zone became widest. The results also indicated that the influence of tidal oscillation on seawater intrusion was restricted only to the region near the coast.

Cheng et al. (1998) used conventional finite element method and a hybrid Lagrangian-Eulerian finite element method to develop a 2-D model (2DFEMFAT) to simulate density-dependent flow and transport through saturated-unsaturated porous media. The model was validated using three test problems. Simulation of two demonstrative examples revealed that the design of withdrawal wells and rates needs to be reassessed. Also, the position of interface is highly dependent on the upland recharge rate and the density difference of saltwater and freshwater.

## 2.5 Comparison of the Sharp Interface and Miscible Transport Modelling Approaches

The earliest analysis of the two approaches is reported by Henry (1960). As mentioned previously (refer Section 2.4 ), on the basis of this analysis Henry concluded that dispersion reduces the extent of seawater intrusion in a coastal aquifer.

Volker and Rushton (1982) presented solutions for a test problem of steady state seawater intrusion in a confined coastal aquifer, under homogeneous and isotropic conditions, using both the sharp interface and miscible transport modelling approaches. Solutions for miscible transport were obtained using the constant dispersion coefficient. The numerical results demonstrated that for large values of constant dispersion coefficient, the miscible transport solution developed a prominent transition zone; with the average position (taken as the position of 0.5 isochlor) of the seawater front significantly different from the position of sharp interface. However, for smaller values of constant dispersion coefficient, the miscible transport solution approached the sharp interface solution. The authors reported the same general trends for velocity-dependent dispersion coefficient.

Hill (1988) simulated steady state seawater intrusion in a cross-section of the layered aquifer system of Cape May County, New Jersey, using the quasi-3-D sharp interface model SHARP (Essaid, 1986) and the 2-D miscible transport model SUTRA (Voss and Souza, 1987). It was found that the location of saltwater in the aquifer system as estimated by SHARP was further landward than that estimated by SUTRA. Hill hypothesized that this difference in solutions was due to an assumption made in the SHARP model concerning vertical flow. It was assumed in the model that leakage through confining beds into an aquifer was small compared to the water in that aquifer and, therefore, due to instantaneous mixing of the two fluids, freshwater leaking into saltwater became part of the saltwater domain and vice versa. This assumption of complete mixing, although reasonable for low rates of leakage, led to inaccurate results for significant amounts of vertical flow in the system. Essaid (1990) modified the model to include restricted mixing of freshwater and saltwater. Simulation using the restricted mixing demonstrated that the interface position

remained unchanged for the uppermost unconfined aquifer while in the lower two aquifers the position of sharp interface was nearer to the 0.5 zone (zone between 0.4 and 0.6 isochlors). However, the slope of the sharp interface and the slopes of isochlors remained different. Also, the toe of the sharp interface in the lower most aquifer remained landward of the 0.5 zone. Essaid reasoned that this difference in the solutions was present because the sharp interface approach does not reproduce the circulation of saltwater in the transition zone.

In an interesting study, Pinder and Stohoff (1988) investigated the transient response of an areal sharp interface model. They simulated a test problem for saltwater upconing beneath a pumping well using both a 2-D areal sharp interface formulation and a 3-D miscible transport formulation. The two simulations yielded entirely different solutions. From the above analysis, the investigators concluded that the assumptions inherent in the vertically integrated sharp interface formulation led to equations which did not accurately represent the dynamics of freshwater-saltwater flow for the test problem considered in the study. It was further concluded that the transient behaviour of regimes exhibiting significant vertical flow cannot be adequately accounted for in the 2-D areal sharp interface formulation.

It is to be noted that upto now, in the author's knowledge, no attempt has been made to analyse the effect of salinewater recharge on the dynamics of a coastal aquifer.

### **3.0 MODEL DEVELOPMENT**

#### **3.1 Problem Definition**

The present study is aimed at developing a numerical model for simulating 2-D (vertical plane) regional transient saltwater transport in a heterogeneous, anisotropic, confined coastal aquifer. Mechanisms of the transport accounted for in the model are advection and hydrodynamic dispersion.

### 3.2 Governing Equations

The problem has been formulated in terms of the following coupled equations:

- i. Equation of solute transport through a porous medium.
- ii. Equation of flow of variable density fluid through a porous medium.
- iii. Constitutive equation relating the density of fluid to its concentration.

#### Solute Transport

The partial differential equation governing 2-D unsteady state solute transport in x-z plane is written as follows (Bear, 1979):

$$\frac{\partial}{\partial x} \left[ \phi \left( D_{xx} \frac{\partial c}{\partial x} + D_{xz} \frac{\partial c}{\partial z} \right) \right] + \frac{\partial}{\partial z} \left[ \phi \left( D_{zx} \frac{\partial c}{\partial x} + D_{zz} \frac{\partial c}{\partial z} \right) \right] - q_x \frac{\partial c}{\partial x} - q_z \frac{\partial c}{\partial z} + W(c^* - c) = \phi \frac{\partial c}{\partial t} \quad (10)$$

where x and z are horizontal and vertical directions, respectively; t is time;  $q_x$  and  $q_z$  are the Darcy velocities in the x- and z- directions, respectively;  $\phi$  is porosity; W is the source/sink volume flux per unit volume of porous medium (+ve sign for inflow);  $D_{xx}$ ,  $D_{xz}$ ,  $D_{zx}$  and  $D_{zz}$  are the coefficients of hydrodynamic dispersion; c and  $c^*$  are, respectively, the dimensionless concentrations of the mixed fluid and the source/sink fluid. These represent, respectively, the volume of seawater per unit volume of groundwater and the source/sink fluid. As is obvious from the above, c and  $c^*$  can range from 0 (freshwater) to 1 (seawater).

The hydrodynamic dispersion coefficients  $D_{xx}$ ,  $D_{xz}$ ,  $D_{zx}$  and  $D_{zz}$  for an isotropic porous medium are defined as follows (Bear, 1979)

$$D_{xx} = \alpha_L \frac{v_x^2}{|v|} + \alpha_T \frac{v_y^2 + v_z^2}{|v|} + D_0 \quad (11a)$$



$$D_{zz} = \alpha_L \frac{v_z^2}{|v|} + \alpha_T \frac{v_x^2 + v_y^2}{|v|} + D_0 \quad (11b)$$

$$D_{xz} = D_{zx} = (\alpha_L - \alpha_T) \frac{v_x v_z}{|v|} \quad (11c)$$

where  $\alpha_L$  and  $\alpha_T$  are the longitudinal and transverse dispersivities, respectively, of an isotropic porous medium;  $D_0$  is coefficient of molecular diffusion;  $v_x$  and  $v_z$  are the components of seepage velocity; and  $|v| = \sqrt{(v_x^2 + v_z^2)}$ .

### Fluid Flow

Keeping in view the time and space variation of the fluid density, the flow equation is expressed in terms of fluid pressure. The partial differential equation governing 2-D, unsteady state flow of a fluid in the x-z plane, accounting for the space and time variations of specific weight and viscosity caused by the concentration variations, is written as follows :

$$\frac{\partial}{\partial x} \left( \frac{\kappa_x \gamma}{\mu} \frac{\partial p}{\partial x} \right) + \frac{\partial}{\partial z} \left[ \frac{\kappa_z \gamma}{\mu} \left( \frac{\partial p}{\partial z} + \gamma \right) \right] + W \gamma^* = S_s \frac{\partial p}{\partial t} \quad (12a)$$

where  $p$  is the fluid pressure;  $\kappa_x$  and  $\kappa_z$  are the intrinsic permeabilities in the x- and z-directions, respectively;  $\gamma$  is the specific weight of fluid;  $S_s$  is the specific storage of porous medium;  $\mu$  is the dynamic viscosity of fluid; and  $\gamma^*$  is the specific weight of source or sink fluid.

The Darcy velocities in x and z directions are given by

$$q_x = - \frac{\kappa_x}{\mu} \frac{\partial p}{\partial x} \quad (12b)$$

$$q_z = - \frac{\kappa_z}{\mu} \left( \frac{\partial p}{\partial z} + \gamma \right) \quad (12c)$$

### Constitutive Equation

For dilute solutions under isothermal conditions, density is treated as a linear function of concentration. The constitutive equation relating the specific weight of fluid to concentration is written as (Frind, 1982a; Huyakorn et al., 1987)

$$\gamma(c) = \gamma_f \left[ 1 + c \left( \frac{\gamma_s}{\gamma_f} - 1 \right) \right] \quad (13)$$

where  $\gamma_s$  is the specific weight of seawater and  $\gamma_f$  is the specific weight of freshwater.

### 3.3 Solution Domain

The domain of solution is taken as a rectangular two-dimensional vertical cross section of a single-layered confined coastal aquifer, of length  $L$  and depth  $D$  as shown schematically in Fig. 1. On one side the domain is exposed to a seawater body. This boundary is referred to as the seaward side. On the other side, referred to as the landward side, the domain is recharged by a freshwater inflow.

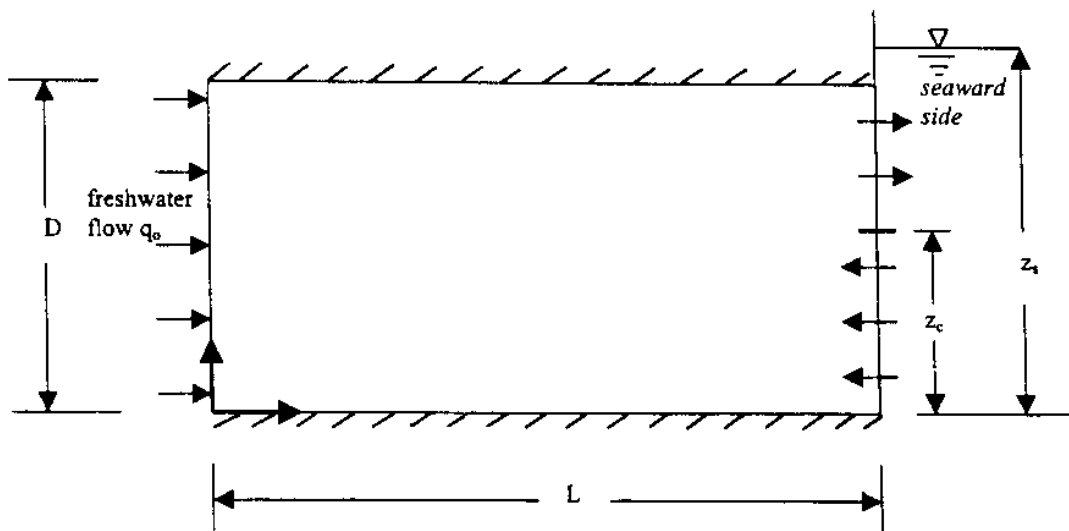


Fig. 1: Solution Domain

### 3.4 Coordinate System

The model employs the x-z coordinate system. The z-coordinate represents the vertical distance from the lower boundary at which it has a zero value. The x-coordinate represents the horizontal distance from the left boundary at which it has a zero value.

### 3.5 Initial and Boundary Conditions for Saltwater Transport

To obtain a unique solution to the transport equation (Eq. (10)) and the flow equation (Eq. (12a)), initial and boundary conditions are specified over the solution domain. For transport equation the initial and boundary conditions considered are as follows:

#### Initial Condition

The domain is initially considered to be saturated with fluid of known concentration distribution. The initial condition is assigned as

$$c(x,z,0) = c(x,z); \quad 0 \leq z \leq D, \quad 0 \leq x \leq L \quad (14)$$

where  $c$  is specified concentration distribution.

#### Boundary Conditions (refer Fig. 1)

##### (a) Seaward Boundary

The boundary on seaward side is a mixed boundary allowing outflow of fluid and inflow of seawater. Accordingly, this boundary is divided into an outflow seaward boundary and an inflow seaward boundary.

i. *Outflow Seaward Boundary*

The outflow boundary on the seaward side allows the advective transport of fluid out of the domain. Assuming that the advective flux in the direction normal to the boundary is the same on both the sides of the boundary, the boundary condition is assigned as (Frind, 1982a)

$$\frac{\partial c}{\partial x} = 0; \quad x = L, z_c < z \leq D, t > 0 \quad (15a)$$

where  $z_c$  is the length of the segment along which inflow boundary is defined as shown in Fig. 1. This length varies with time depending upon the direction of flow along the seaward boundary.

ii. *Inflow Seaward Boundary*

For the vertical inflow boundary on the seaward side, the boundary condition is assigned as

$$c = 1; \quad x = L, 0 \leq z \leq z_c, t > 0 \quad (15b)$$

It is obvious that the respective distances along which the inflow boundary and outflow boundary are defined do not remain constant but depend upon the segment length ' $z_c$ ' which varies with time depending upon the direction of flow along the seaward boundary. The two boundaries are defined, accordingly, by first ascertaining the segment length  $z_c$  on seaward boundary along which the flow is directed inward and marking it as the inflow boundary. The remaining portion of the seaward boundary is marked as the outflow boundary or 'window'. The segment length  $z_c$  is updated for each iteration cycle as the simulation progresses with time.

(b) *Bottom Impervious Boundary*

The bottom boundary is the impervious boundary across which the total flux of seawater is zero. The boundary condition is assigned as

$$\frac{\partial c}{\partial z} = 0; \quad 0 < x < L, z = 0, t > 0 \quad (15c)$$

(c) *Landward Boundary*

Across the boundary on the landward side there is a freshwater flux into the domain. Therefore, the boundary condition is of the form

$$c = 0; \quad x = 0, 0 \leq z \leq D, t > 0 \quad (15d)$$

(d) *Top impervious boundary*

For the top impervious boundary, the boundary condition is assigned as

$$\frac{\partial c}{\partial z} = 0; \quad 0 < x < L, z = D, t > 0 \quad (15e)$$

### 3.6 Initial and Boundary Conditions for Fluid Flow

#### Initial Condition

The initial condition is assigned, by considering a known initial pressure distribution, as follows:

$$p(x,z,0) = p(x,z); \quad 0 \leq z \leq D, 0 \leq x \leq L \quad (16)$$

where  $p$  is a specified pressure distribution.

#### Boundary Conditions (refer Fig. 1)

(a) *Seaward Boundary*

The seaward boundary is subject to hydrostatic pressure distribution as follows:

$$p = \gamma_s (z_s - z); \quad x = L, 0 \leq z \leq D, t > 0 \quad (17a)$$

where  $z_s$  is the mean sea level.

*(b) Bottom Impervious Boundary*

The bottom impervious boundary defines the lower boundary of the solution domain. Since there is no flow normal to an impervious layer, the boundary condition is assigned as

$$\frac{\partial p}{\partial z} = 0; \quad 0 < x < L, z = 0, t > 0 \quad (17b)$$

*(c) Landward Boundary*

Considering a uniform distribution of freshwater inflow over the depth  $D$ , and in a direction normal to the boundary, the boundary condition is assigned as

$$\frac{\kappa_x}{\mu} \frac{\partial p}{\partial x} = -q_o; \quad x = 0, 0 \leq z \leq D, t > 0 \quad (17c)$$

where  $q_o$  is the specified freshwater flow.

*(d) Top Impervious Boundary*

The top impervious boundary defines the upper boundary of the solution domain. The boundary condition is assigned as

$$\frac{\partial p}{\partial z} = 0; \quad 0 < x < L, z = D, t > 0 \quad (17d)$$

### **3.7 The Solution Strategy**

The transport equation (Eq. (10)) and the flow equation (Eq. (12a)) are coupled through constitutive equation (Eq. (13)) and Darcy's equations (Eqs. (12b) and (12c)) in a manner which renders them nonlinear. In the present study, the solute transport equation and the fluid flow equation are solved using the Iterative Alternating Direction Implicit (IADI) scheme of finite differences. During each iteration, the IADI method generates a tridiagonal system of equations, which is solved using the Thomas algorithm (Remson et al., 1978).

Density coupling of the flow and transport equations is handled using a Picard sequential solution algorithm with provision for automatic reduction of time step values when the stipulated number of iterations is exceeded

Initially, the solute transport equation is solved using IADI scheme and the necessary velocity components are taken in accordance with the initial steady state condition. The value of specific weight is updated using Eq. (13), which is then used to compute the pressure distribution by solving the fluid flow equation. The individual velocity components needed for the solution of transport equation are computed using Darcy's law for variable density fluid flow (Eqs. (12b) and (12c)). Subsequently, the transport and flow equations are solved and a convergence check is performed to determine if successive changes in pressure and concentration are within prescribed tolerances. If the convergence criterion is not met, the flow and transport equations are solved using updated values of pressure and concentration. Updating of the pressure and concentration values is performed by updating the specific weight distribution. Subsequent iterations are carried out until the prescribed convergence criterion is satisfied or the maximum stipulated number of iterations is exceeded. If convergence of the solution is obtained, computations are carried out for the next time level. If the solution fails to converge within the maximum number of iterations, then the time step value is reduced by half and the above steps for solution of flow and transport equations are repeated. The process continues until convergence is achieved or the stipulated number of iterations is exceeded. Thus, the solution of transport equation coupled with flow equation yields the spatial distribution of concentration over various discrete time steps (refer Appendix I).

#### **4.0 MODEL VALIDATION**

The numerical model was validated by comparing the simulated results with the previously published numerical solution (Voss and Souza, 1987) of Henry's Problem (1964) and the semi-analytical solution given by Henry.

## 4.1 Henry's Problem

As described in Section 2.4, the problem addresses seawater intrusion in a confined coastal aquifer under steady flow conditions. The problem domain consisting of a rectangular, homogeneous, isotropic aquifer, bounded on top and bottom by impervious boundaries, is exposed to a seawater body on one side and receives a constant freshwater flux from the other side. The problem assumes a constant dispersion coefficient and no window on the seaward side.

### 4.1.1 Model Operation

The model was operated neglecting the existence of window on seaward side and using a constant dispersion coefficient. The length and depth of the solution domain was taken as 2.0 m and 1.0 m respectively. A mesh-centered finite difference grid of 11 rows and 21 columns was superposed over the solution domain.

To reproduce Henry's Problem, the parameter values (Frind, 1982a) listed in Table 1 were adopted.

*Table 1 Parameter Values for Henry's Problem*

Parameter	Value	Parameter	Value
$\alpha_L$	0.0	$\phi$	0.35
$\alpha_T$	0.0	$g$	9.81 m/s <sup>2</sup>
$\kappa_x$	1.04412*10 <sup>-9</sup> m <sup>2</sup>	$\rho_s$	1024.5 kg/m <sup>3</sup>
$\kappa_z$	1.04412*10 <sup>-9</sup> m <sup>2</sup>	$\rho_f$	1000 kg/m <sup>3</sup>
$S_s$	0.0	$\mu$	1*10 <sup>-3</sup> kg/m-s
$q_0$	6.6*10 <sup>-5</sup> m/s	$D_0$	6.6*10 <sup>-6</sup> m <sup>2</sup> /s



These values reproduced Henry's parameters as follows:

$$k_1 = K \frac{\rho_s - \rho_f}{\rho_f} = \frac{\kappa \rho_f g}{\mu} \frac{\rho_s - \rho_f}{\rho_f}$$

$$= \frac{1.044126 * 10^{-9} * 1000 * 9.81}{1 * 10^{-3}} * \frac{1024.5 - 1000}{1000}$$

$$= 2.509505 * 10^{-4} \text{ m/s}$$

$$\xi = l/d = 2/1 = 2.0$$

$$\text{For } Q = q_0 d = 6.6 * 10^{-5} * 1.0 = 6.6 * 10^{-5} \text{ m}^2/\text{s}$$

$$a = \frac{Q}{k_1 d} = \frac{6.6 * 10^{-5}}{2.50905 * 10^{-4}} = 0.263$$

$$b = \frac{D}{Q} = \frac{6.6 * 10^{-6}}{6.6 * 10^{-5}} = 0.1$$

It should be noted that Henry's Problem assumes a constant dispersion coefficient. To simulate a constant value of dispersion coefficient through the present model,  $\alpha_L$  and  $\alpha_T$  were assigned a zero value while the molecular diffusion coefficient  $D_0$  was assigned a value equal to the dispersion coefficient.

Taking the initial freshwater head above the mean sea level as zero, the initial conditions were assigned in accordance with Eqs. (14) and (16).

Boundary conditions for the transport equation were assigned in accordance with Eqs. (15a) - (15e). In accordance with Henry's boundary conditions, the presence of window on seaward side was neglected and the boundary condition was taken as  $c = 1$ . Boundary conditions for the flow equation were assigned in accordance with Eqs. (17a) - (17d).

The model was operated till the system attained steady state. A time step of 24.0 sec was used initially, which was increased to a maximum of 600.0 sec at later times. The simulation was stopped at about 306 min because of the attainment of steady state, which was characterized with insignificant changes in concentration distribution.

#### **4.1.2 Results and Discussion**

Figure 2 shows the family of isochlors (0.1 to 0.9) at steady state. The Ghyben-Herzberg interface computed from the corresponding head profile is also shown superposed over the simulated disperse interface.

In Fig. 3, the 0.5 isochlor (which has been taken to be representative of the average position of disperse interface), computed by the proposed model is compared with numerical solution reported by Voss and Souza (1987) obtained using SUTRA. From the above figure it is evident that the 0.5 isochlor computed using the proposed model is in good agreement with SUTRA solution over the major portion, except the top part. This deviation is primarily due to the different boundary conditions used in the proposed model to simulate Henry's Problem. These are similar to Henry's original boundary conditions.

The steady state position of the disperse interface (Fig. 3) given by Henry's semi-analytical solution appears to overestimate the seawater penetration, as observed by other researchers also (Voss and Souza, 1987; Frind, 1982a). A possible explanation for the differences in the semi-analytical and both the numerical solutions may be the truncation errors in Henry's semi-analytical solution, present due to the missing higher-order terms which were originally dropped for the sake of reducing computation time.

To conclude, none of the numerical solutions successfully match Henry's semi-analytical solution. However, the satisfactory agreement between the present solution and

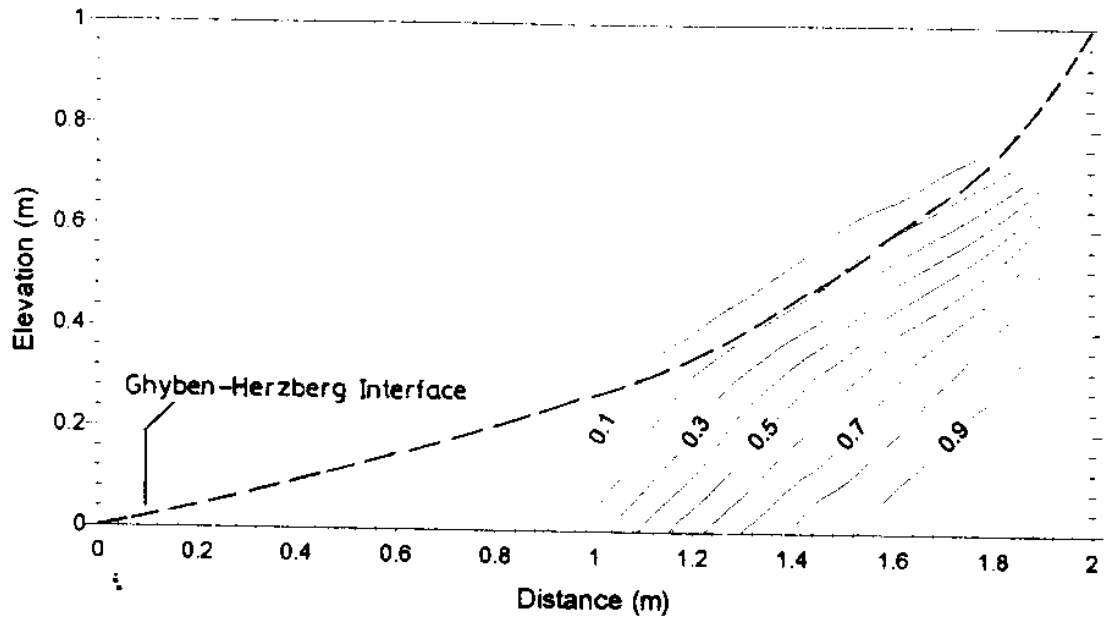


Fig. 2: Concentration distribution at steady state (Henry's Problem)

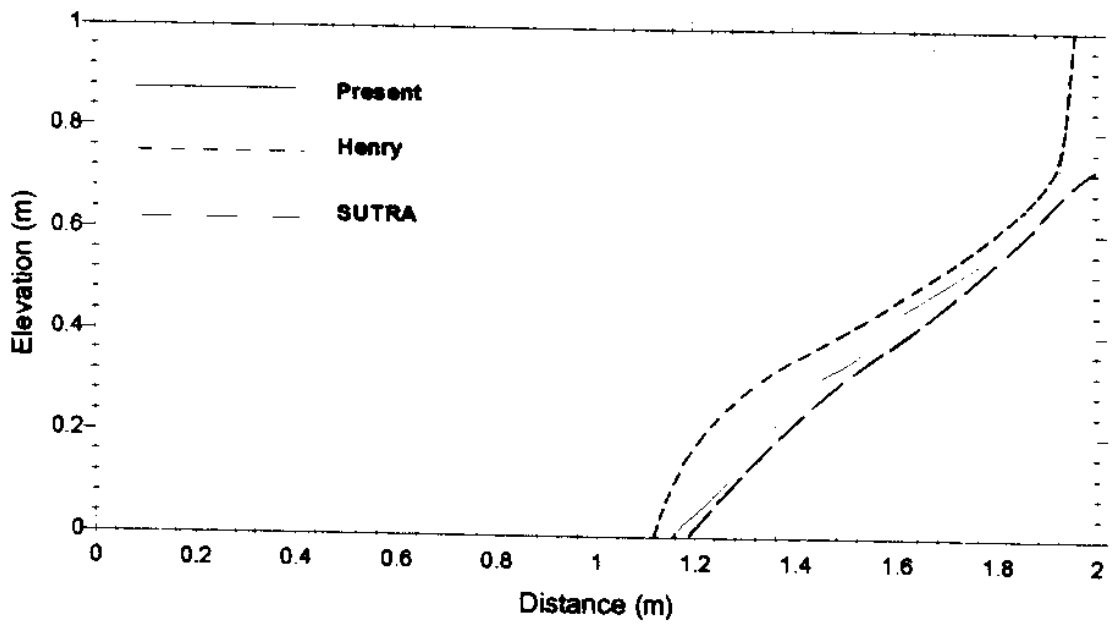


Fig. 3: Comparison of computed 0.5 isochlor with Henry's semi-analytical solution and SUTRA numerical solution

the numerical solution given by the well-known SUTRA model imparts credibility to the present model. The Ghyben-Herzberg interface does not agree well with the corresponding disperse interface simulated by the model (Fig. 2). The toe of the Ghyben-Herzberg interface lies much further inland mainly because Ghyben-Herzberg solution does not account for the circulation caused by dispersion.

## **5.0 MODEL APPLICATION**

As mentioned in Section 1.0, in addition to lateral intrusion of saltwater from the adjacent sea, the freshwater aquifers on the eastern coast of India are vulnerable to contamination from other sources as well. The gently sloping surface of the coastline repeatedly gets flooded with salinewater during cyclonic storms. The widespread adoption of aquaculture by farmers has resulted in the proliferation of aquaculture tanks over large tracts of land near the coast, especially in Andhra Pradesh. Aquaculture is basically the technique of artificial propagation of animals and plants in water. Broad classes of organisms grown include fish, plants, reptiles, crustaceans and mollusks destined for food or non-food markets. Production systems include ponds, tanks, net pens, suspended cages, and the net bags and bottom nets used on submerged lands for clam production. Water quality may range from fresh through brackish to salinity exceeding seawater.

In Andhra Pradesh, mostly prawn is being cultivated, which requires salinewater for growth. The water quality in these aquaculture tanks usually ranges from brackish to seawater. The submergence of land under a blanket of salinewater due to both these factors, i.e., cyclonic storms and aquaculture tanks, results in a vertical recharge of salinewater to the underlying freshwater aquifer. In this way, the coastal aquifer is subject to both seawater intrusion and a vertical recharge of saline water from the top.

In the present study an attempt has been made to examine the behaviour of a coastal aquifer system, when it is subject to a vertical recharge of saline water due to infiltration of salinewater from aquaculture tanks as well as flooding of the low-lying coastal areas with salinewater during cyclonic storms. The present model has been used to simulate the dynamics of coastal aquifers under the above condition for different possible scenarios using hypothetical data. For this purpose, the model was initially used to simulate a hypothetical problem, which was originally used by Huyakorn et al. in 1987 to simulate saltwater transport in an unconfined coastal aquifer. Later on, this problem is modified in order to investigate different scenarios pertaining to vertical recharge of salinewater.

### 5.1 Hypothetical Problem

As proposed by Huyakorn et al., this problem addresses seawater intrusion in an anisotropic unconfined coastal aquifer receiving a constant vertical and lateral freshwater recharge (Fig. 4).

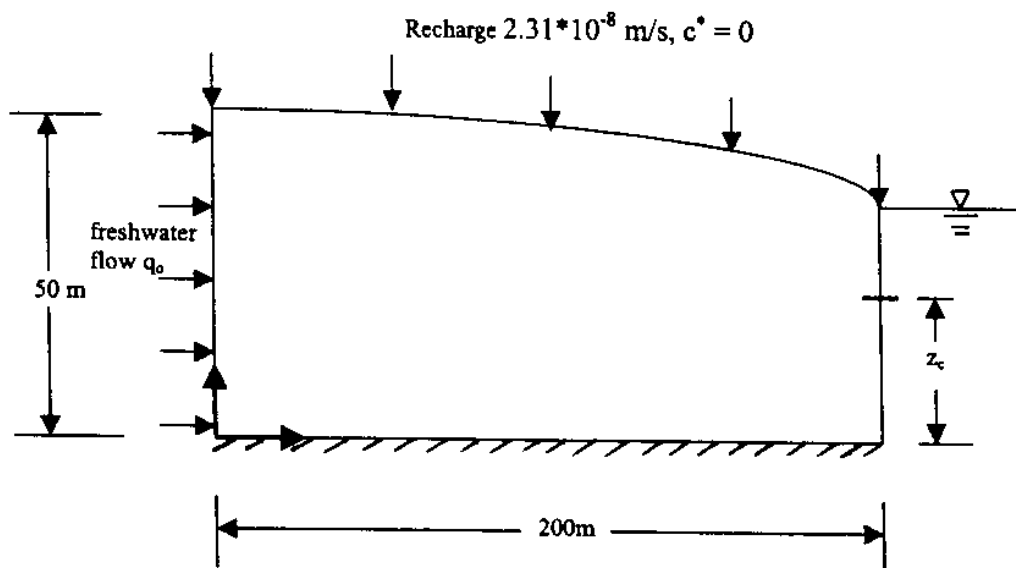


Fig. 4: Definition sketch of hypothetical problem

Considering a solution domain of size 200 m x 50 m, Huyakorn et al. assumed the following parameter values:

$$K_x = 4.0 \text{ m/d} \quad (\kappa_x = 4.719296 \cdot 10^{-12} \text{ m}^2 \text{ for } \rho_f = 1000 \text{ kg/m}^3, \mu = 1.0 \cdot 10^{-3} \text{ kg/m-s});$$

$$K_z = 0.4 \text{ m/d} \quad (\kappa_z = 4.719296 \cdot 10^{-13} \text{ m}^2 \text{ for } \rho_f = 1000 \text{ kg/m}^3, \mu = 1.0 \cdot 10^{-3} \text{ kg/m-s});$$

$$q_o = 4 \cdot 10^{-3} \text{ m/d} \quad (= 4.63 \cdot 10^{-8} \text{ m/s}); \quad \alpha_L = 10 \text{ m}; \quad \alpha_T = 5 \text{ m};$$

$$\phi = 0.25; \quad \varepsilon = (\rho_s - \rho_f)/\rho_f = 0.025, \quad g = 9.81 \text{ m/s}^2$$

The vertical recharge was taken equal to  $2 \cdot 10^{-3} \text{ m/d}$  ( $= 2.31 \cdot 10^{-8} \text{ m/s}$ ). The boundary conditions used by Huyakorn et al., which provide for the existence of window, were based on a constant saturated thickness of the unconfined aquifer and a fixed depth (30 m) of window below mean sea level (msl).

The initial conditions included zero values of hydraulic head and concentration. The numerical solution reported by Huyakorn et al. gives the position of 0.5 isochlor at steady state and a maximum head build-up approximately equal to 1.05 m.

### 5.1.1 Model Operation

A finite difference grid consisting of 6 rows and 21 columns was superposed over the solution domain of size 200m x 50 m. The model, accounting for varying depth of window and ignoring the domain above the msl, was operated using the parameter values noted above.

The initial conditions were assigned in accordance with Eqs. (14) and (16). The boundary conditions for transport and flow equations were assigned in accordance with Eqs. (15a) - (15e) and (17a) - (17d), respectively. The top boundary of the model, which was earlier taken to be an impervious boundary for the confined case, was modified to account for the vertical recharge. However, during the simulation, the position of this free surface boundary was fixed at an elevation of 50 m above the base of the unconfined aquifer. Although, this is a rather approximate way to treat the free surface condition, it is reasonable

for the present problem because the maximum rise in the water table due to recharge has been reported by Huyakorn et al. to be about 1.05 m, which is only 2.1% of the saturated thickness. Thus, the assumption of constant saturated thickness of the unconfined aquifer in the present problem is justified.

The model was operated till the system attained steady state. For the simulation of flow and transport a time step of 15 days was used initially, which was gradually increased to a maximum of 100 days at later times. The near steady state was attained at about 8450 days.

### 5.1.2 Results and Discussion

Figure 5 shows the family of isochlors at steady state produced by the model. For comparison the 0.5 isochlor reported by Huyakorn et al. is shown with a dotted curve. The Ghyben-Herzberg interface is also superposed over the simulated disperse interface, for comparison.

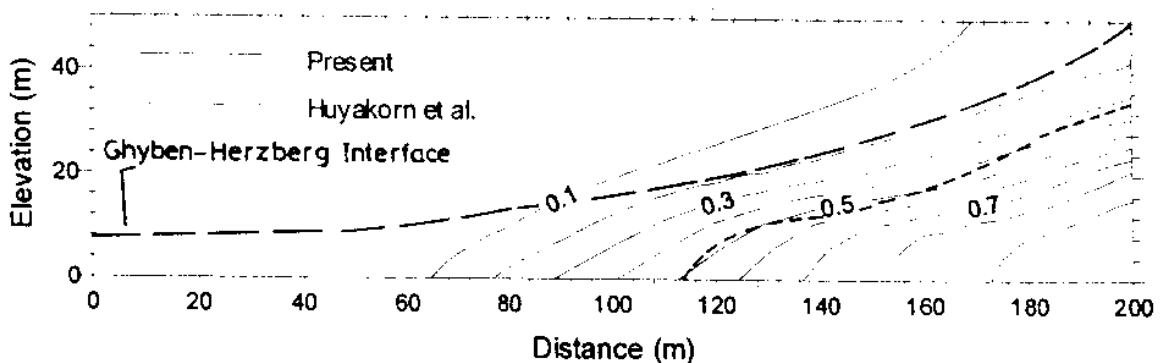


Fig. 5: Concentration distribution at steady state (Hypothetical Problem)

From the figure it is clear that both the numerical solutions are in satisfactory agreement. Again, as was observed in Henry's Problem, the toe of the Ghyben-Herzberg interface intrudes much further inland. This is because Ghyben-Herzberg solution does not account for the circulation caused by dispersion.

## 5.2 Simulation of Hypothetical Scenarios of Vertical Salinewater Recharge

In order to simulate the effect of vertical recharge of salinewater in a coastal aquifer, the problem considered in Section 5.1 was modified. The model was operated in two stages in each of which different scenarios were considered.

### 5.2.1 Model Operation - Stage I

The model was operated, using the parameter values as defined for the problem in Section 5.1, for the following different hypothetical cases:

Case I : Vertical recharge over 25% length of the domain with  $c^* = 0.0, 0.5, 1.0$

Case II : Vertical recharge over 50% length of the domain with  $c^* = 0.0, 0.5, 1.0$

Case III : Vertical recharge over 75% length of the domain with  $c^* = 0.0, 0.5, 1.0$

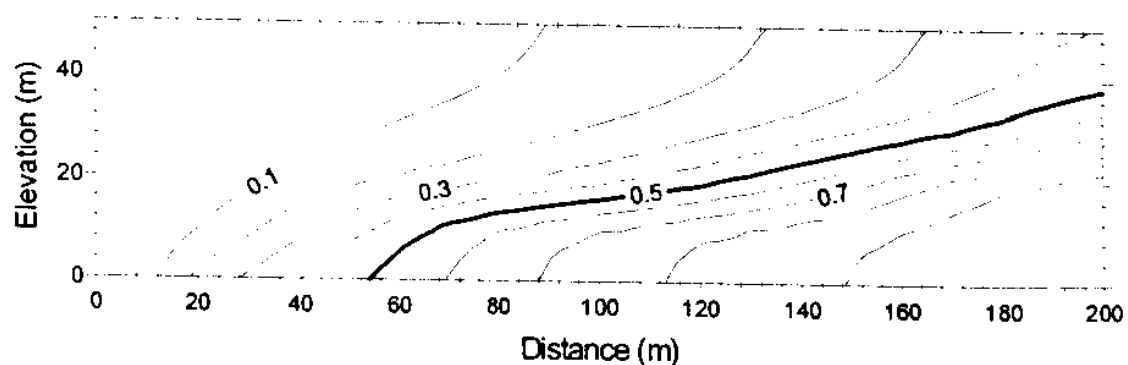
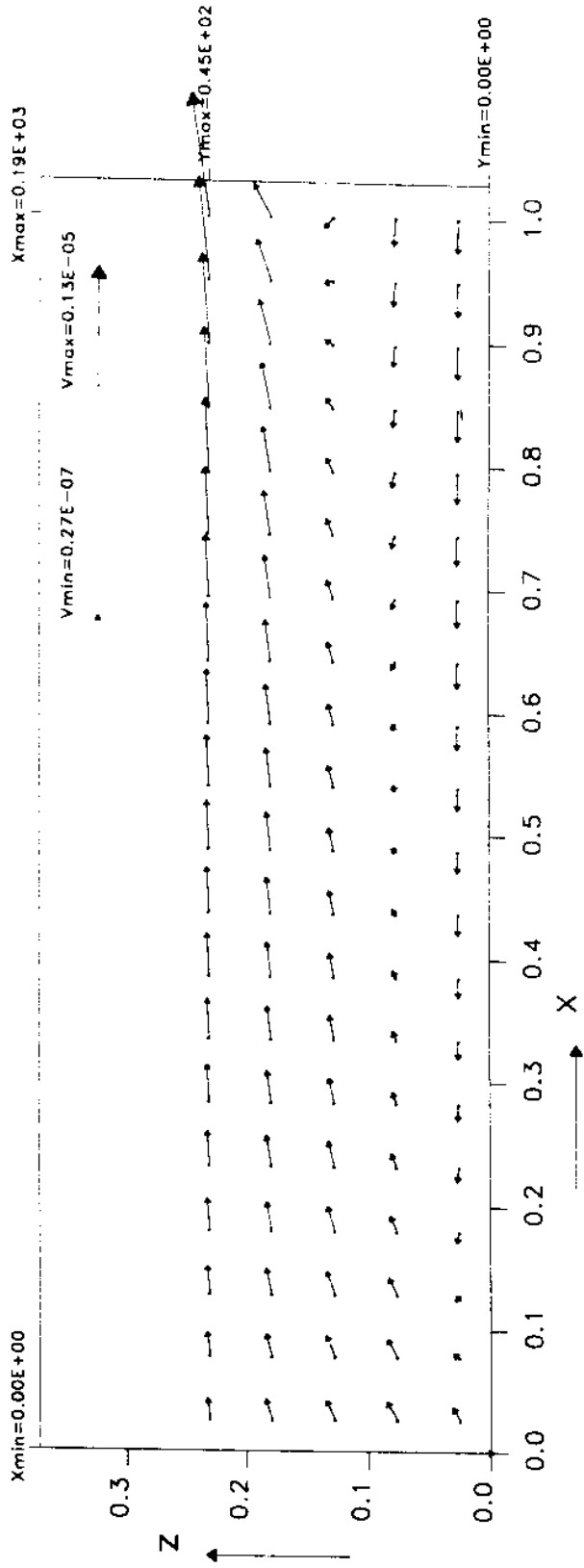


Fig. 6: Concentration distribution at steady state with no vertical recharge (Initial Condition for Stage I)

The steady state concentration and pressure distribution attained on receiving only a lateral freshwater recharge to the unconfined aquifer was taken as the initial condition in all the above cases. The concentration distribution and velocity distribution at the initial state are illustrated in Figs. 6 and 7, respectively. As mentioned previously in Section 5.0, the water quality of an aquaculture tank may vary from freshwater to brine. Therefore, for



Fig. 7: Steady state velocity field with no recharge (Initial Condition for Stage I)

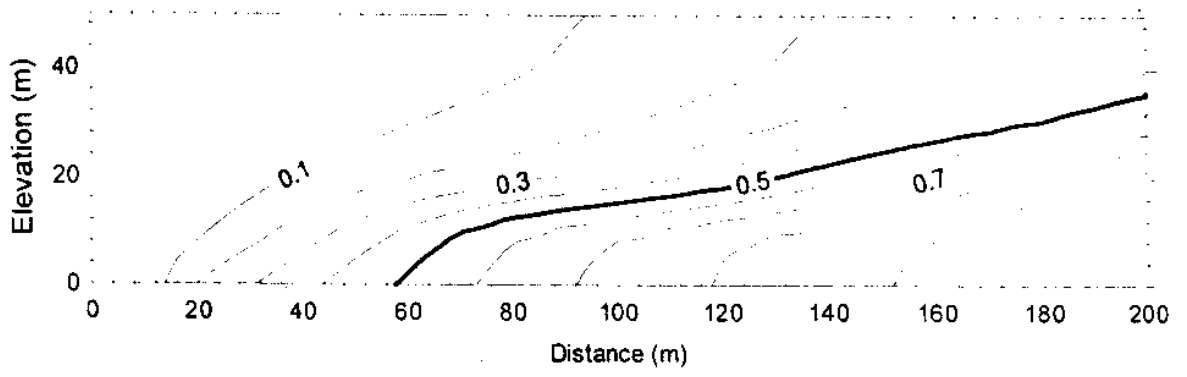


simulating Cases I, II and III, the concentration of recharge fluid at the top surface boundary has been taken to be varying from 0 to 1.

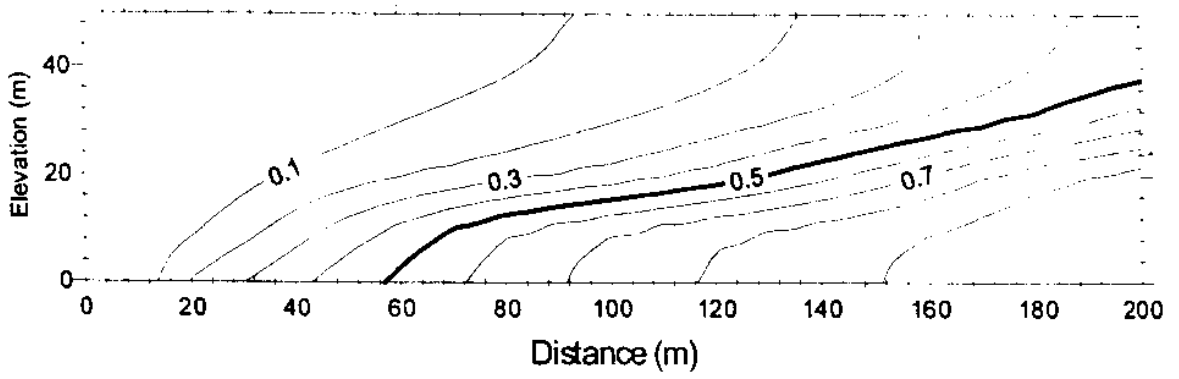
### 5.2.1.1 Results and Discussion

Figures 8(a), 8(b) and 8(c) show the family of isochlors for Case I at steady state. The respective concentration distribution visible in these figures is achieved when the aquifer is subject to a continuous long term recharge. The 0.5 isochlor is shown as a thick curve, since it has been taken to represent the average position of the disperse interface. Similarly, Figs. 9(a), 9(b), 9(c) and 10(a), 10(b), 10(c) show the isochlors at steady state for Cases II and III. From these figures, it can be inferred that the impact of vertical salinewater recharge is maximum in case III with  $c^* = 1$ . However, on comparison with Fig. 6, it is evident that although the position of isochlors at the top of the aquifer has shifted landwards, the position of isochlors at the bottom of aquifer has retreated towards the sea. This is despite the aquifer receiving a vertical salinewater recharge. The retreat of interface is larger in the case of salinewater recharge of lesser concentration (i.e.,  $c^* = 0.5$ ) compared to the case with salinewater recharge of maximum concentration (i.e.,  $c^* = 1$ ). The reason for this retreat in general is the reduction in seawater inflow, as is evident on comparing Figs. 7 and 11. These figures depict the respective velocity fields at initial state and at the steady state acquired w.r.t. Case III with  $c^* = 1$ . The landward inflow of seawater is small when there is vertical recharge of salinewater compared to the case when no recharge is occurring. The maximum outflow velocity of the mixed fluid is slightly more, because of an increase in total recharge to the aquifer.

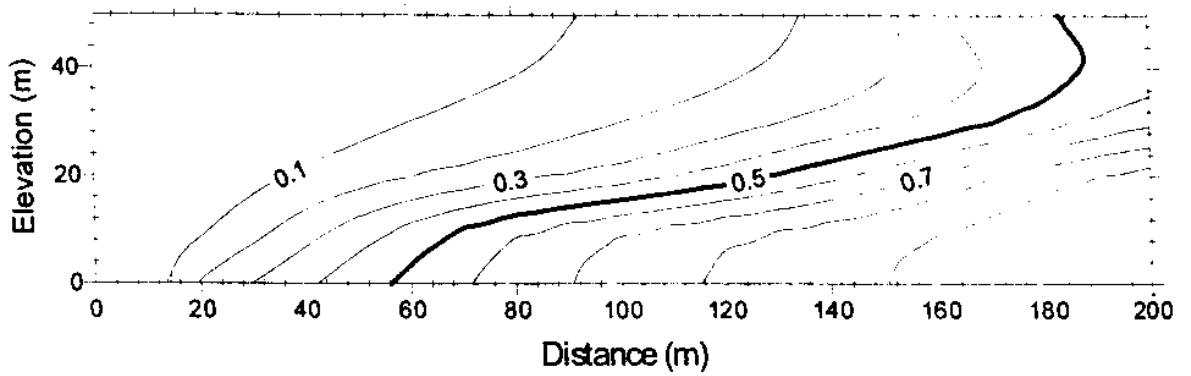
Figures 12(a), 12(b), 12(c) respectively illustrate the transient condition existing in the aquifer after 5, 30, and 90 days of continuously receiving salinewater recharge ( $c^* = 0.5$ ) over 75% length of the domain. On comparison with Fig. 6 it is clear from these figures that the increase in salinity occurs in the upper portion of the aquifer at early times. It is at the later times that the disperse interface at the bottom of the aquifer starts retreating. This is clear on comparison of Fig. 6, which shows the initial concentration distribution, and Figs. 13(a) and 13(b), which show the interface position after 720 and 3960 days.



(a)  $c^* = 0$

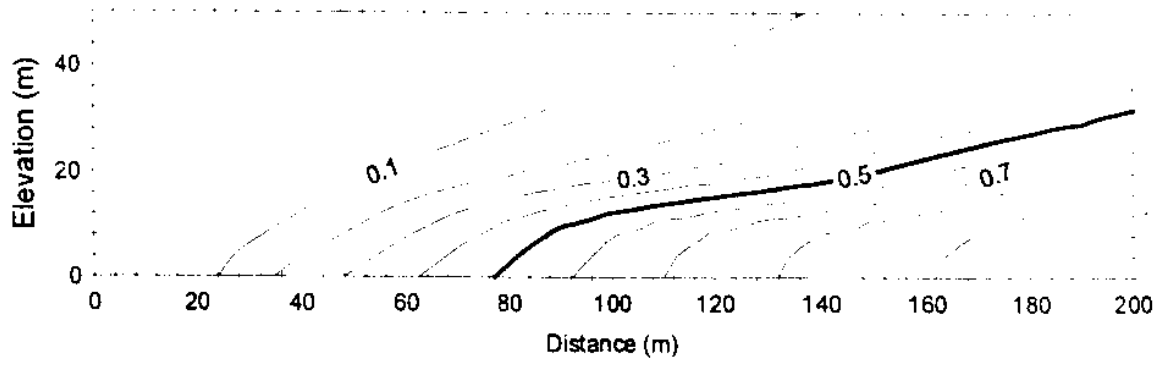


(b)  $c^* = 0.5$

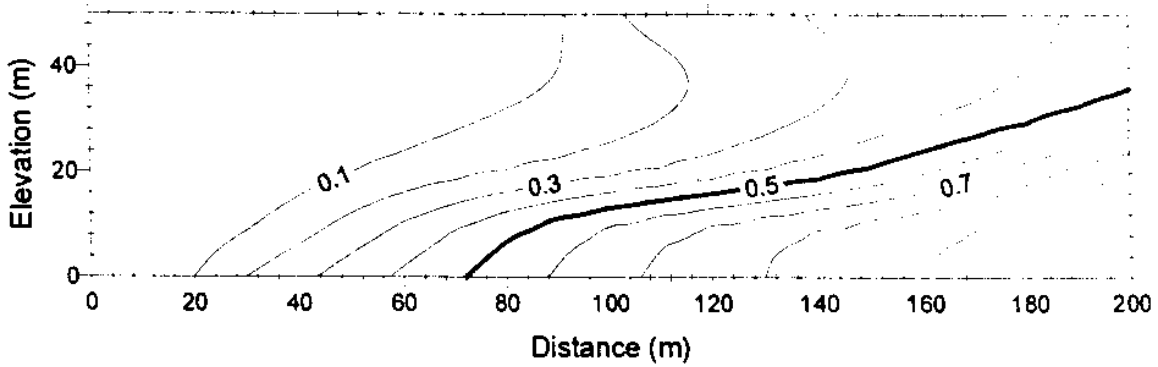


(c)  $c^* = 1$

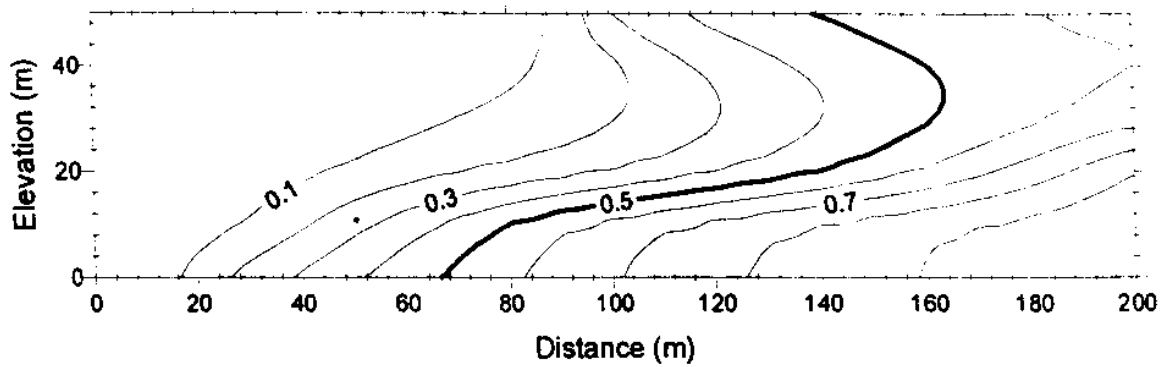
Fig. 8: Concentration distribution at steady state, Stage I - Case I



(a)  $c^* = 0$

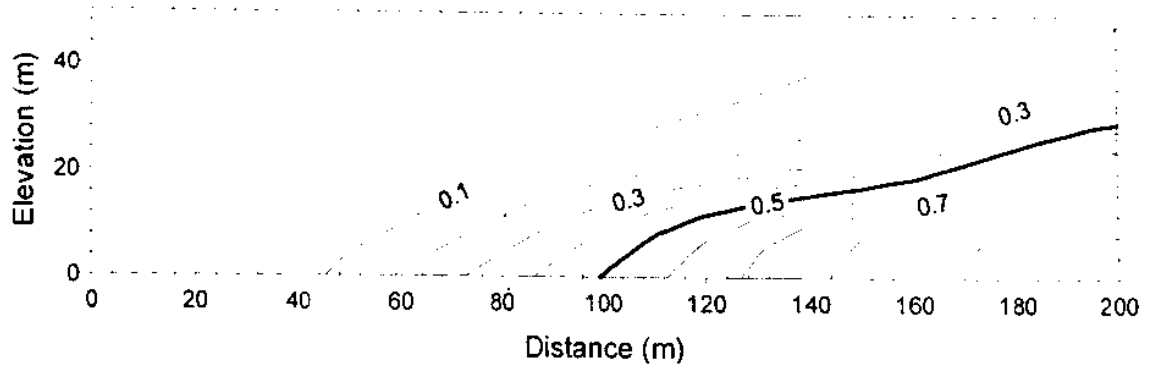


(b)  $c^* = 0.5$

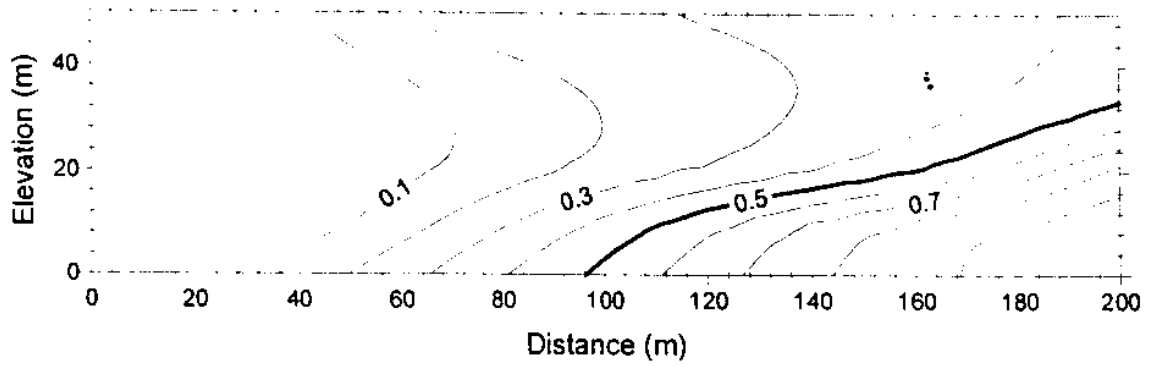


(c)  $c^* = 1$

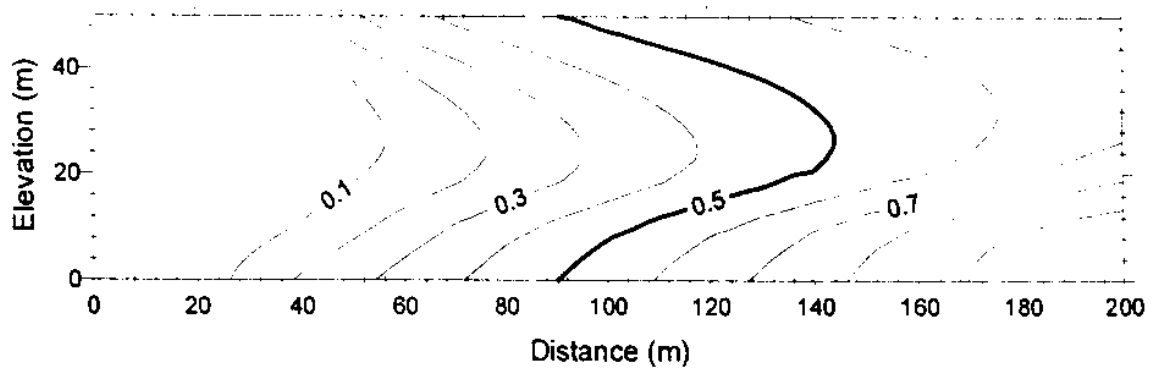
Fig. 9: Concentration distribution at steady state, Stage I - Case II



(a)  $c^* = 0$



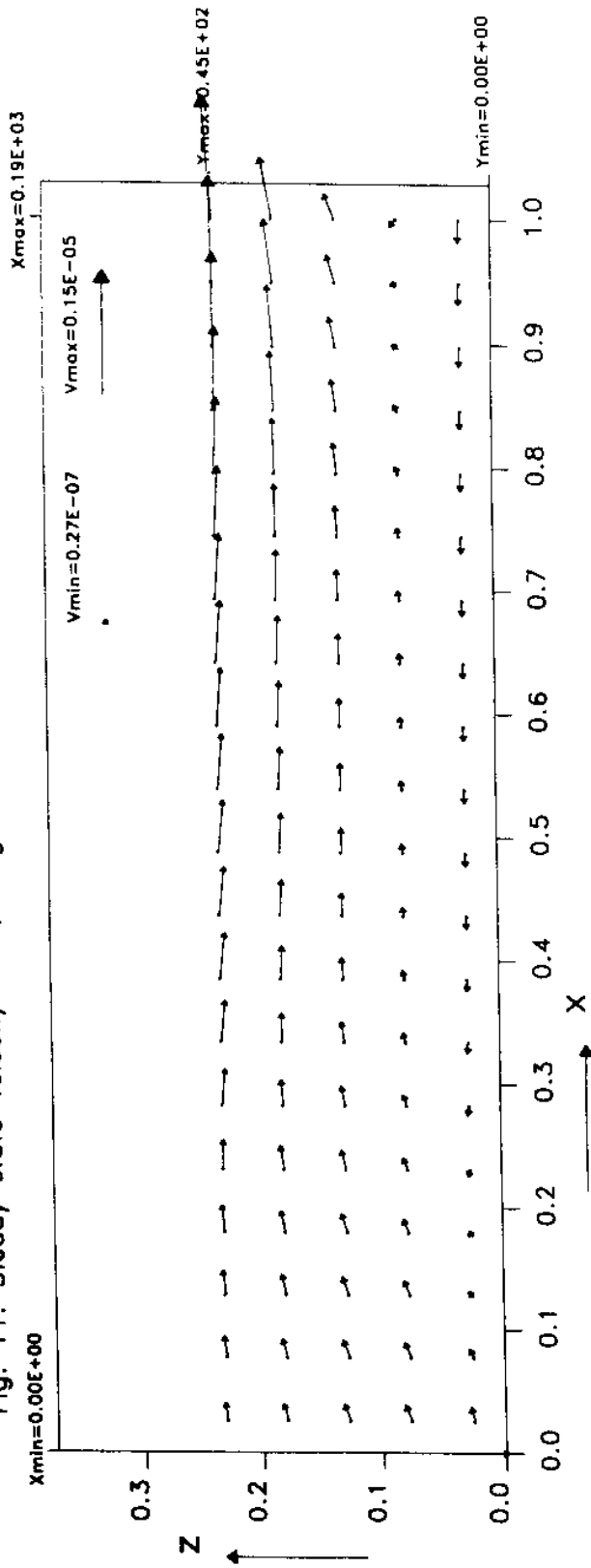
(b)  $c^* = 0.5$

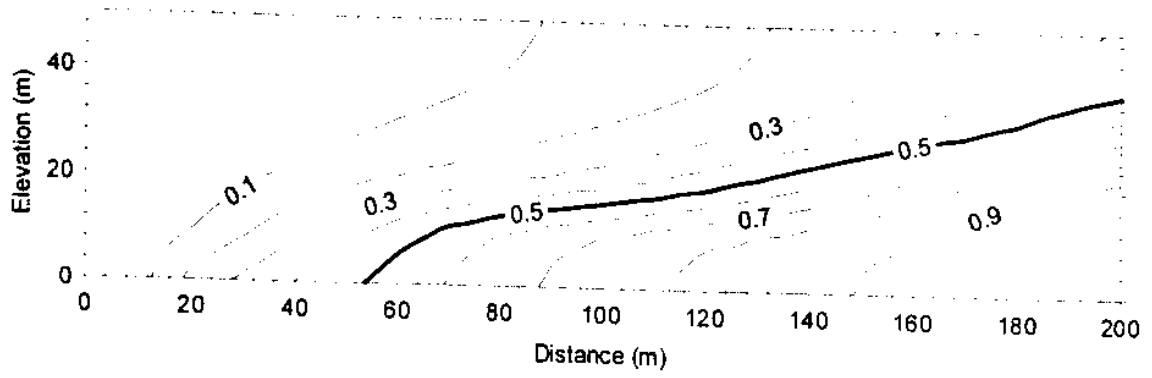


(c)  $c^* = 1$

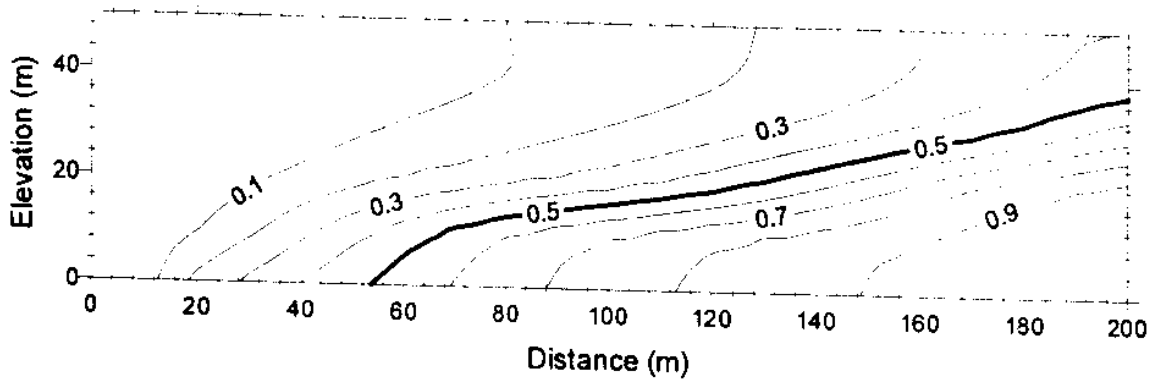
Fig. 10: Concentration distribution at steady state, Stage I - Case III

Fig. 11: Steady state velocity field, Stage I - Case III for  $c^* = 1$

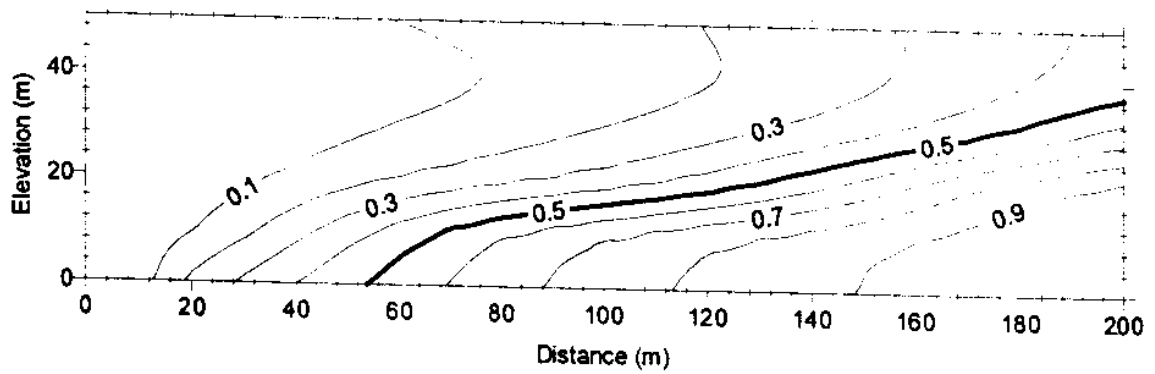




(a) after 5 days

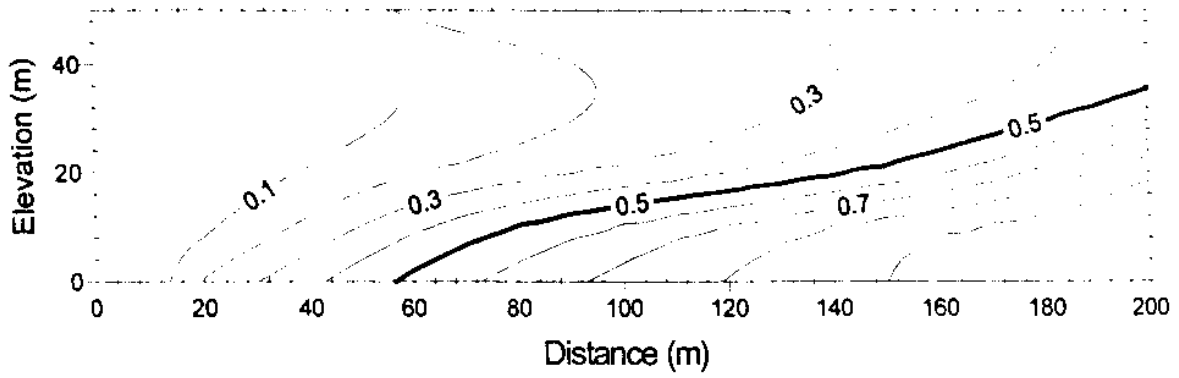


(b) after 30 days

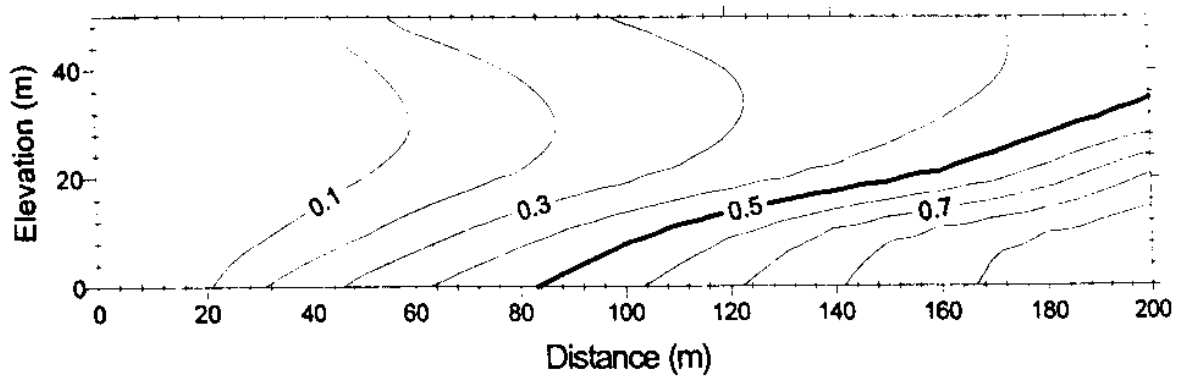


(c) after 90 days

Fig. 12: Concentration distribution with recharge  $c^* = 0.5$ , Stage I - Case III  
(Transient state at early times)



(a) After 720 days



(b) After 3960 days

Fig. 13: Concentration distribution with recharge  $c^* = 0.5$ , Stage I - Case III  
(Transient state at later times)



It is to be noted that for all the cases considered in Stage I, the disperse interface retreats when the aquifer receives freshwater recharge (i.e.,  $c^* = 0$ ). The amount of retreat increases as the area under freshwater recharge increases (refer Figs. 8(a), 9(a) and 10(a)).

## 5.2.2 Model Operation - Stage II

For Stage II, the initial condition was taken to be the steady state attained when the aquifer has been subject to continuous salinewater recharge with  $c^* = 0.5$  over 75% length of domain (refer Fig. 10(b)). Again the initial scenario for the recharge fluid having a concentration of 0.5 has been considered, since it represents the average concentration value in a tank/pond used for aquaculture. Here, the aim was to investigate the movement of interface in response to a freshwater vertical recharge and in absence of recharge with the initial condition defined as above. Thus, the following two cases were analysed :

Case I : Freshwater vertical recharge over 75% length of the domain

Case II : No vertical recharge

### 5.2.2.1 Results and Discussion

On running the simulation for Case I, it was found that some significant shift in the position of isochlors at the top of the aquifer occurs only after about 90 days. Figure 14 shows the concentration distribution in the aquifer after 90 days of continuously receiving freshwater recharge of  $2.31 \cdot 10^{-8}$  m/s. Figure 15 shows the concentration distribution after 90 days in absence of vertical recharge. On comparing Figs. 14 and 15 it is obvious that the retreat of isochlors at the top of the aquifer for Case II is less than Case I. For both cases, there is no change in the position of isochlors at the bottom of aquifer which would occur only at later times.

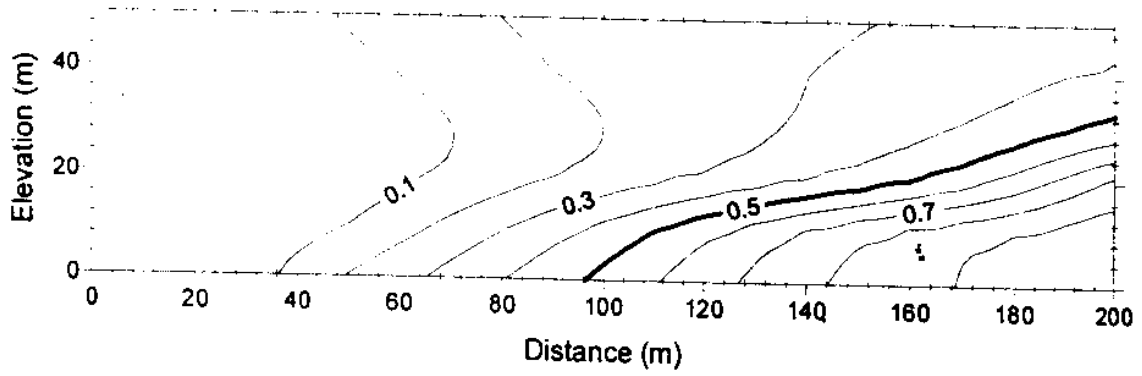


Fig. 14: Concentration distribution after 90 days, Stage II - Case I

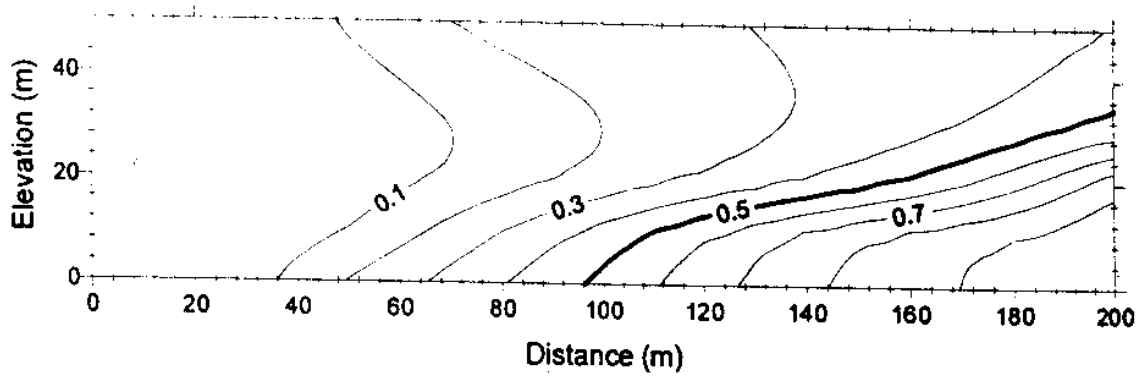
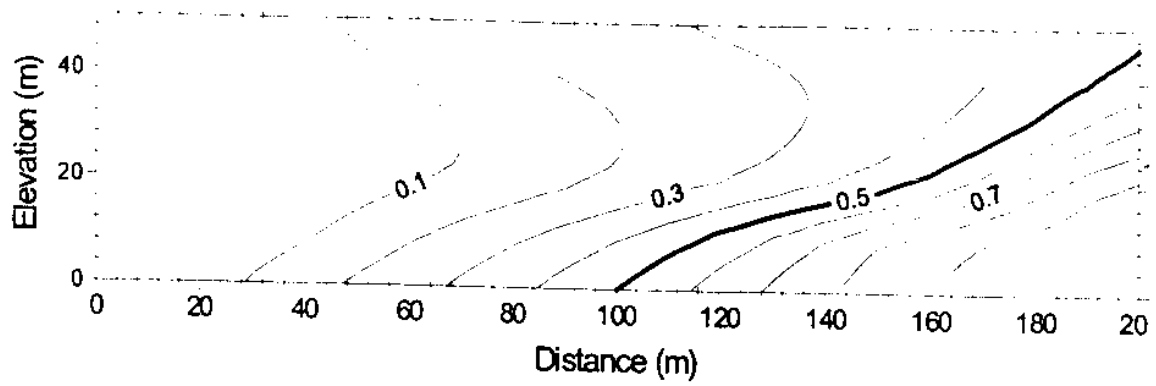


Fig. 15: Concentration distribution after 90 days, Stage II - Case II

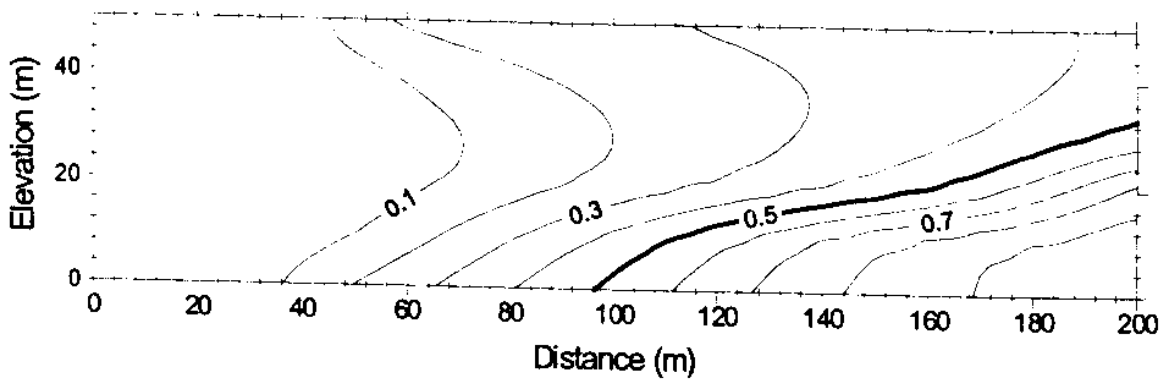
### 5.3 Effect of Anisotropy on Salinewater Recharge

To investigate the effect of anisotropy on salinewater recharge to the underlying aquifer, the  $\kappa_x/\kappa_z$  ratio was varied as 2, 10, and 50. The recharge of  $2.31 \cdot 10^{-8}$  m/s with  $c^* = 0.5$  was taken to be occurring over 75% length of the domain. The initial condition was taken to be the same as for Stage I (refer Section 5.2.1). Figures 16(a), 16(b), 16(c) show the concentration distribution at steady state, for respective values of  $\kappa_x/\kappa_z$ . Figures 17(a) and 17(b) illustrate the respective velocity fields existing at steady state for  $\kappa_x/\kappa_z = 2$  and  $\kappa_x/\kappa_z = 50$ .

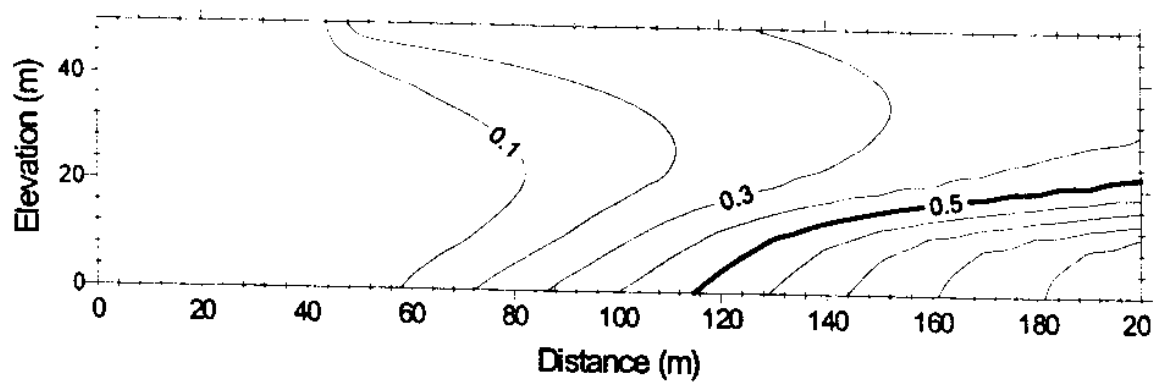
From these figures, it is clear that although the tips of isochlors 0.1 and 0.2, which represent smaller values of concentration advance landwards slightly, the toes of all the isochlors retreat seawards as anisotropy increases. Moreover, all the isochlors representing concentration values greater than 0.4 tend to become flat as anisotropy increases. The reason behind this pattern of change in the position of isochlors, as anisotropy increases, is clear on comparing Figs. 17(a) and 17(b). The inflow of seawater for  $\kappa_x/\kappa_z = 2$  is more pronounced compared to that for  $\kappa_x/\kappa_z = 50$ . Also, the reversal of landward flow of seawater back towards the sea occurs much further inland for  $\kappa_x/\kappa_z = 2$ , which explains larger penetration of seawater in this case. The low value of vertical permeability in case of  $\kappa_x/\kappa_z = 50$  accounts for the small magnitude of vertical velocity component which in turn gives rise to the flattened shape of isochlors in Fig. 16(c). In all, larger values of velocities in Fig. 17(a) lead to larger values of dispersion coefficients and greater amount of seawater circulation for  $\kappa_x/\kappa_z = 2$ , compared to  $\kappa_x/\kappa_z = 50$ .



(a) for anisotropy = 2



(b) for anisotropy = 10



(c) for anisotropy = 50

Fig. 16: Effect of anisotropy on saline water recharge: Concentration distribution at steady state with recharge  $c^* = 0.5$  over 75% length of domain

Fig. 17(a): Steady state velocity field with recharge  $c^* = 0.5$  over 75' length of domain, anisotropy = 2

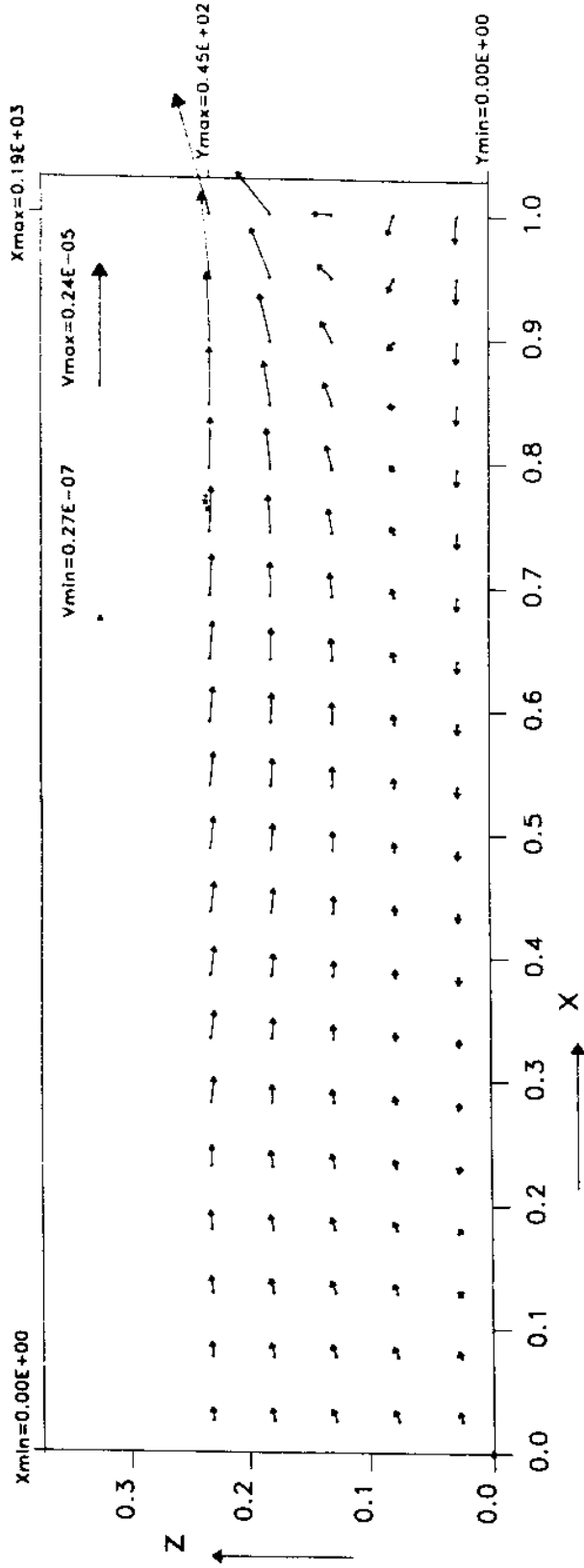
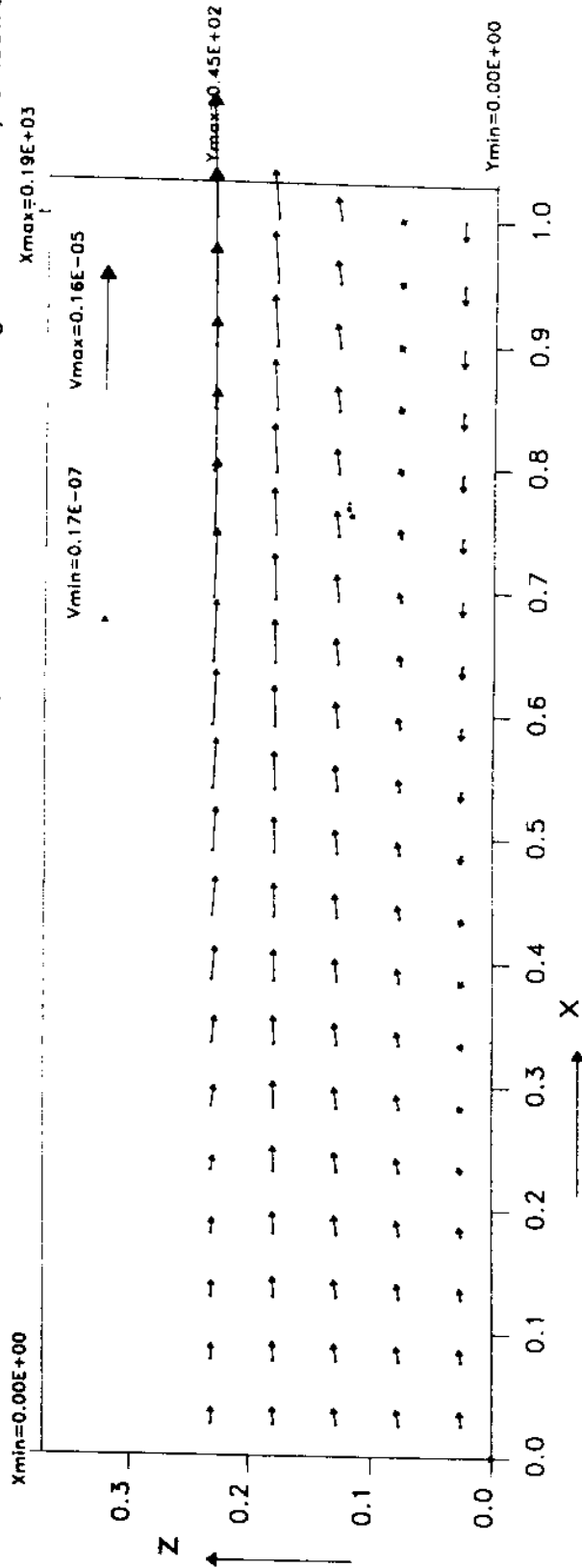


Fig. 17(b): Steady state velocity field with recharge  $c^* = 0.5$  over 75' length of domain, anisotropy = 50



## 6.0 CONCLUSIONS

A 2-D numerical model in the vertical plane to simulate regional transient saltwater transport in a heterogeneous, anisotropic confined coastal aquifer has been developed. The model is based on the miscible transport approach, which accounts for saltwater transport due to both advection and hydrodynamic dispersion. The governing equations are solved using the IADI technique of finite differences. The model has been validated by comparing the computed solution with the reported semi-analytical solution and SUTRA numerical solution of Henry's Problem. The model with modified upper boundary condition has been applied to evaluate the effect of vertical salinewater recharge on the dynamics of an unconfined coastal aquifer by simulating different hypothetical scenarios involving both short-term and long-term vertical recharge of salinewater to an unconfined aquifer. The results show that continuous salinewater recharge increases salinity levels in the upper portion of the aquifer at early times (i.e., after a few months). The increase is largest for maximum concentration of recharge fluid and for recharge occurring over a large area. At later times, despite the aquifer receiving a salinewater recharge, the disperse interface at the bottom of the aquifer retreats because of the increase in total recharge to the aquifer. This retreat is smallest for maximum concentration of recharge fluid. For freshwater recharge, the retreat increases as the area of recharge increases.

For an unconfined aquifer which has been initially subject to continuous salinewater recharge, the introduction of freshwater recharge results in retreat of the interface at the top of the aquifer at early times. This retreat is faster compared to the case when no recharge occurs.

For identical values of salinewater recharge, an aquifer with lower value of anisotropy exhibits larger seawater penetration and seawater circulation compared to an aquifer with a higher value of anisotropy.

Thus, continuous salinewater recharge raises the salinity levels mainly in the upper portion of the aquifer. This rise in salinity depends on the area of recharge and concentration

of recharge fluid. The natural dynamic equilibrium existing between freshwater and seawater in a coastal aquifer is significantly disturbed if a large area is subject to salinewater recharge. Therefore, aquaculture practice which results in salinewater recharge to the underlying aquifer should be restricted to narrow regions along the coastal belt and the salinity in aquaculture tanks should be kept low.

## References

- Badon Ghyben, W., (1888), 'Nota in verband met de voorgenomen putboring nabij Amsterdam (Notes on the probable results of well drilling near Amsterdam)', Tijdschr. Kon. Inst. Ing., The Hague, pp. 8-22.
- Bear, J., (1979), 'Hydraulics of ground water', McGraw-Hill, New York, 569 pp.
- Bear, J. and Dagan, G., (1964a), 'Some exact solutions of interface problems by means of the hodograph method', J. Geophys. Res., Vol. 69, No.8, pp.1563-1572.
- Bear, J. and Dagan, G., (1964b), 'Moving interface in coastal aquifer,' J. Hydraul. Div., Proc. ASCE, Vol. 90, No. HY4, pp. 193-216.
- Bush, P.W., (1988), 'Simulation of saltwater movement in the Floridan aquifer system, Hilton Head Island, South Carolina', U.S. Geol. Surv. Water-Supply Pap. 2331, 19 pp.
- Cheng, Jing-Ru, Strobl, R.O., Yeh, G-Tsyh, Lin, H-Chi and Choi, W.H., (1998), 'Modelling of 2D density-dependent flow and transport in the subsurface', J. Hydrol. Eng., ASCE, Vol. 3, No. 4, pp. 248-257.
- Cooper, H.H., Kohout, F.A., Henry, H.R. and Glover, R.E., (1964), 'Sea water in coastal aquifers', U.S. Geol. Surv. Water-Supply Pap. 1613-C, 84 pp.
- Eem, J.P. van der, (1992), 'Calculation methods for local variable density ground water problems', In: Study and Modelling of Saltwater Intrusion into Aquifers, Proc. 12 Saltwater Intrusion Meeting (E. Custodio and A. Galofre, eds.), Barcelona, Spain, pp. 437-451.
- Essaid, H.I., (1986), 'A comparison of the coupled fresh water-salt water flow and the Ghyben-Herzberg sharp interface approaches to modeling of transient behaviour in coastal aquifer systems', J. Hydrol., Vol. 86, pp. 169-193.
- Essaid, H.I., (1990), 'The computer model SHARP, a quasi-three-dimensional finite difference model to simulate freshwater and saltwater flow in layered coastal aquifer systems', U.S. Geol. Surv. Water-Resour. Invest. Rep. 90-4130, 181 pp.



- Frind, E.O., (1982a), 'Simulation of long-term transient density-dependent transport in groundwater', *Adv. Water Resour.*, Vol.5, pp. 73-88.
- Frind, E.O., (1982b), 'Seawater intrusion in continuous coastal aquifer aquitard systems', *Adv. Water Resour.*, Vol. 5, pp. 89-97.
- Garder, A.O., Jr., Peaceman, D.W. and Pozzi, A.L., Jr., (1964), 'Numerical calculation of multidimensional miscible displacement by the method of characteristics', *Soc. Petrol. Eng. J.*, Vol. 4, No. 1, pp. 26-36.
- Galeati, G., Gambolati, G. and Neuman, S.P., (1992), 'Coupled and partially coupled Eulerian-Lagrangian model of freshwater-seawater mixing', *Water Resour. Res.*, Vol. 28, No. 1, pp. 149-165.
- Glover, R.E., (1959), 'The pattern of fresh-water flow in a coastal aquifer', *J. Geophys. Res.*, Vol. 64, No. 4, pp. 457-459.
- Gupta, A.D. and Sivanathan, N., (1988), 'Modelling of sea water intrusion of layered coastal aquifer', *Proc. 7 Int. Conf. on Computational Methods in Water Resour., Developments in Water Science 35, Vol. 1 - Modeling surface and sub-surface flows*, (M.A. Celia, L.A. Ferrand, C.A. Brebbia, W.G. Gray and G.F.Pinder, eds.) MIT, pp. 205-210.
- Henry, H.R., (1959), 'Salt intrusion into fresh water aquifers', *J. Geophys. Res.*, Vol. 64, No.11, pp. 1911-1919.
- Henry, H.R., (1960), 'Salt intrusion into coastal aquifers', *Int. Assoc. Sci. Hydrol., Publ. No. 52*, pp. 478-487.
- Henry, H.R., (1964), 'Effect of dispersion on salt encroachment in coastal aquifers', In: *Sea Water in Coastal Aquifers*, U.S. Geol. Surv., Water-Supply Pap. 1613-C, pp. 70-84.
- Herzberg, A., (1901), 'Die wasserversorgung einiger Nordseebaden (The water supply on parts of the North Sea Coast)', *J. Gasbeleucht. Wasserversorg.*, Vol.44, pp. 815-819, 842-844.
- Hill, M.C., (1988), 'A comparison of coupled freshwater-saltwater sharp interface and convective-dispersive models of saltwater intrusion in a layered aquifer system', *Proc. 7 Int. Conf. on Computational Methods in Water Resour., Developments in Water Science 35, Vol. 1 - Modeling surface and sub-surface flows*, (M.A. Celia, L.A. Ferrand, C.A. Brebbia, W.G. Gray and G.F. Pinder, eds.), MIT, pp. 211-216.
- Hubbert, M.K., (1940), 'The theory of ground water motion', *J. Geol.*, Vol. 48, No.8, pp. 785-944.
- Huyakorn, P.S., Andersen, P.F., Mercer, J.W., and White, H.O., Jr., (1987), 'Saltwater intrusion in aquifers: development and testing of three-dimensional finite element model', *Water Resour. Res.*, Vol. 23, No. 2, pp. 293-312.

- Huyakorn, P.S. and Panday, S., (1990), 'DSTRAM documentation and user's guide', Code Documentation Report, Hydrogeologic, Inc., Herndon, VA, Code Doc. Rep., 170 pp.
- Inouchi, K., Kishi, Y. and Kakinuma, T., (1990), 'The motion of coastal groundwater in response to the tide', *J. Hydrol.*, Vol. 115, pp. 165-191.
- Intercomp Resource Development and Engineering, Inc., (1976), 'A model for calculating effects of liquid waste disposal in deep saline aquifers, Parts I and II', U.S. Geol. Surv. Water-Resour. Invest. 76-61, 253 pp.
- Intera, (1979), 'Revision of the documentation for a model for calculating effects of liquid waste disposal in deep saline aquifers', U.S. Geol. Surv. Water-Resour. Invest. 79-96, 73 pp.
- Kipp, K.L., Jr., (1987) 'HST3D: A computer code for simulation of heat and solute transport in three-dimensional groundwater flow systems', U.S. Geol. Surv. Water-Resour. Invest. Rep. 86-4095, 515 pp.
- Kipp, K.L., Jr., (1997) 'Guide to the revised heat and solute transport simulator: HST3D-Version 2', U.S. Geol. Surv. Water-Resour. Invest. Rep. 97-4157, 148 pp.
- Mercer, J.W., Larson, S.P. and Faust, C.R., (1980), 'Simulation of salt-water interface motion', *Ground Water*, Vol. 18, No. 4, pp. 374-385.
- Mahesha, A., (1995), 'Parametric studies on the advancing interface in coastal aquifers due to linear variation of the freshwater level', *Water Resour. Res.*, Vol. 31, No. 10, pp. 2437-2442.
- Mahesha, A., (1996), 'Control of seawater intrusion through injection-extraction well system', *Technical Notes, J. Irrig. and Drain. Eng.*, ASCE, Vol. 122, No. 5, pp. 314-317.
- Ogata, A. and Banks, R.B., (1961), 'A solution of the differential equation of longitudinal dispersion in porous media', U.S. Geol. Surv. Professional Pap. 411-A, 7 pp.
- Panday, S., Huyakorn, P.S., Robertson, J.B. and McGurk, B., (1993), 'A density-dependent flow and transport analysis of the effects of groundwater development in a freshwater lens of limited areal extent: The Geneva area (Florida, U.S.A.) case study', *J. Contam. Hydrol.*, Vol. 12, pp. 329-354.
- Pinder, G.F. and Gray, W.G., (1977), 'Finite element simulation in surface and subsurface hydrology', Academic Press, New York, 295 pp.
- Pinder, G. and Stohoff, S., (1988), 'Can the sharp interface salt-water model capture transient behaviour?', *Proc. 7 Int. Conf. on Computational Methods in Water Resour., Developments in Water Science 35*, Vol. 1 - Modeling surface and sub-surface flows, (M.A. Celia, L.A. Ferrand, C.A. Brebbia, W.G. Gray and G.F. Pinder, eds.), MIT, pp. 217-222.

Remson, I., Hornberger, G.M., and Molz, F.J., (1971), 'Numerical methods in subsurface hydrology', John Wiley, New York, 389 pp.

Reilly, T.E., (1990), 'Simulation of dispersion in layered coastal aquifer system', J. Hydrol., Vol. 114, pp. 211-228.

Rouve, G. and Stoessinger, W., (1980), 'Simulation of the transient position of the saltwater intrusion in the coastal aquifer near Madras coast', Proc. 3 Int. Conf. on Finite Elements in Water Resour. (S.V. Wang, C.A. Brebbia, C.V. Alonso, W.G. Gray and G.F. Pinder, eds.), Univ. of Mississippi, Miss., pp. 2.219-2.228.

Sharma, A., (1996), 'Numerical modelling of seawater transport in coastal aquifers', Ph.D. Thesis, Dept. of Hydrology, University of Roorkee, Roorkee

Smith, B.S., (1994), 'Saltwater movement in the upper Floridan aquifer beneath Port Royal Sound, South Carolina', U.S. Geol. Surv. Water-Supply Pap. 2421, 40 pp.

Souza, W.R. and Voss, C.I., (1987), 'Analysis of an anisotropic coastal aquifer system using variable-density flow and solute transport simulation', J. Hydrol., Vol. 92, pp. 17-41.

Spitz, F.J., and Barringer, T.H., (1992), 'Ground-water hydrology and simulation of saltwater encroachment, shallow aquifer system of southern Cape May County, New Jersey', U.S. Geol. Surv. Water-Resour. Invest. Rep. 91-4191, 87 pp.

Volker, R.E. and Rushton, K.R., (1982), 'An assessment of the importance of some parameters for seawater intrusion in aquifers and a comparison of dispersive and sharp-interface modelling approaches', J. Hydrol., Vol. 56, pp. 239-250.

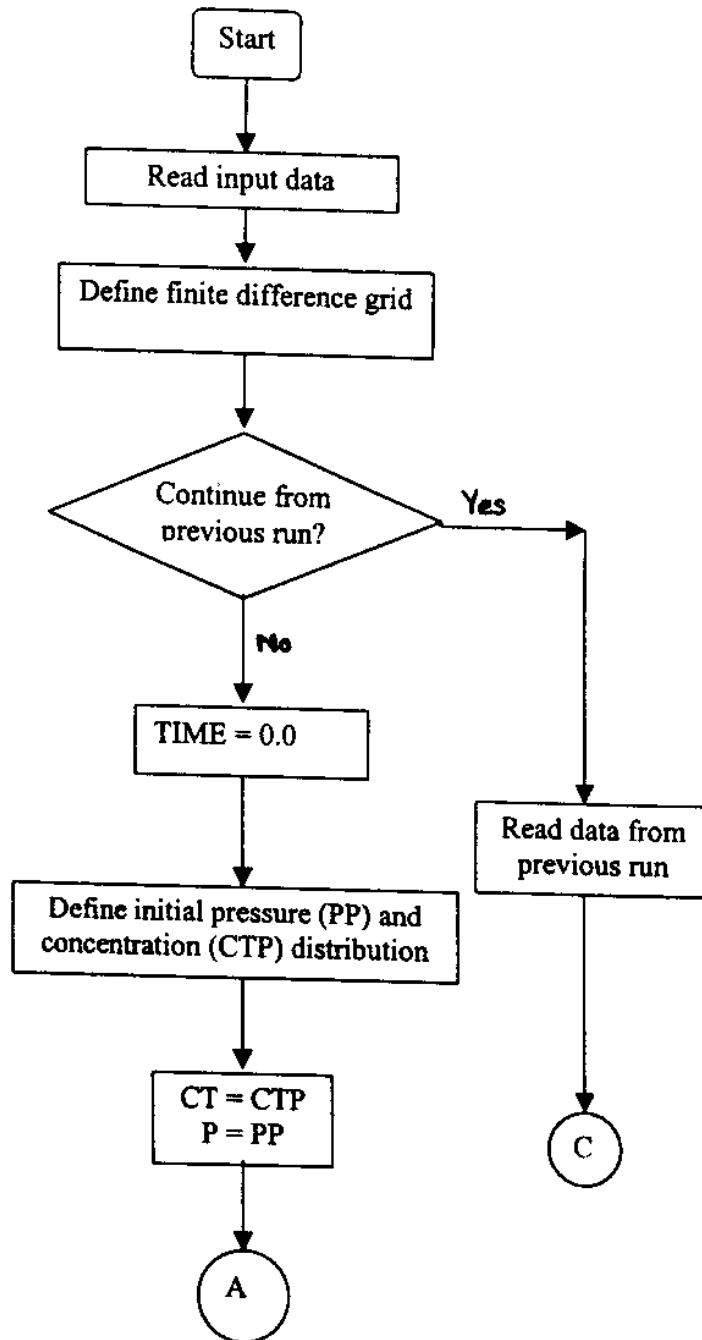
Voss, C.I., (1984), 'A finite-element simulation model for saturated-unsaturated fluid-density-dependent groundwater flow with energy transport or chemically-reactive single-species solute transport', U.S. Geol. Surv. Water Resour. Invest. Rep. 84-4369, 409 pp.

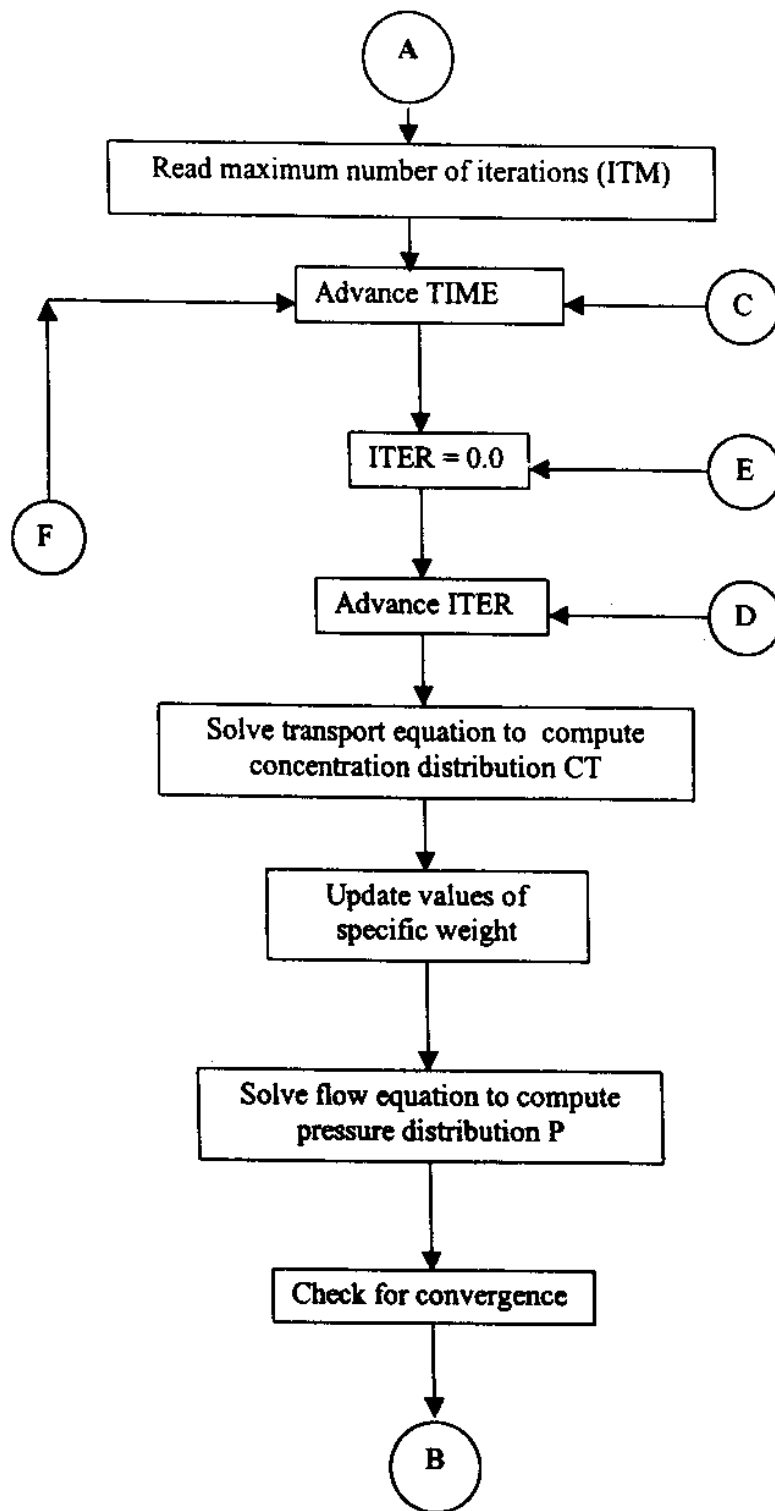
Voss, C.I. and Souza, W.R., (1987), 'Variable density flow and solute transport simulation of regional aquifers containing a narrow freshwater-saltwater transition zone', Water Resour. Res., Vol. 23, No. 10, pp. 1851-1866.

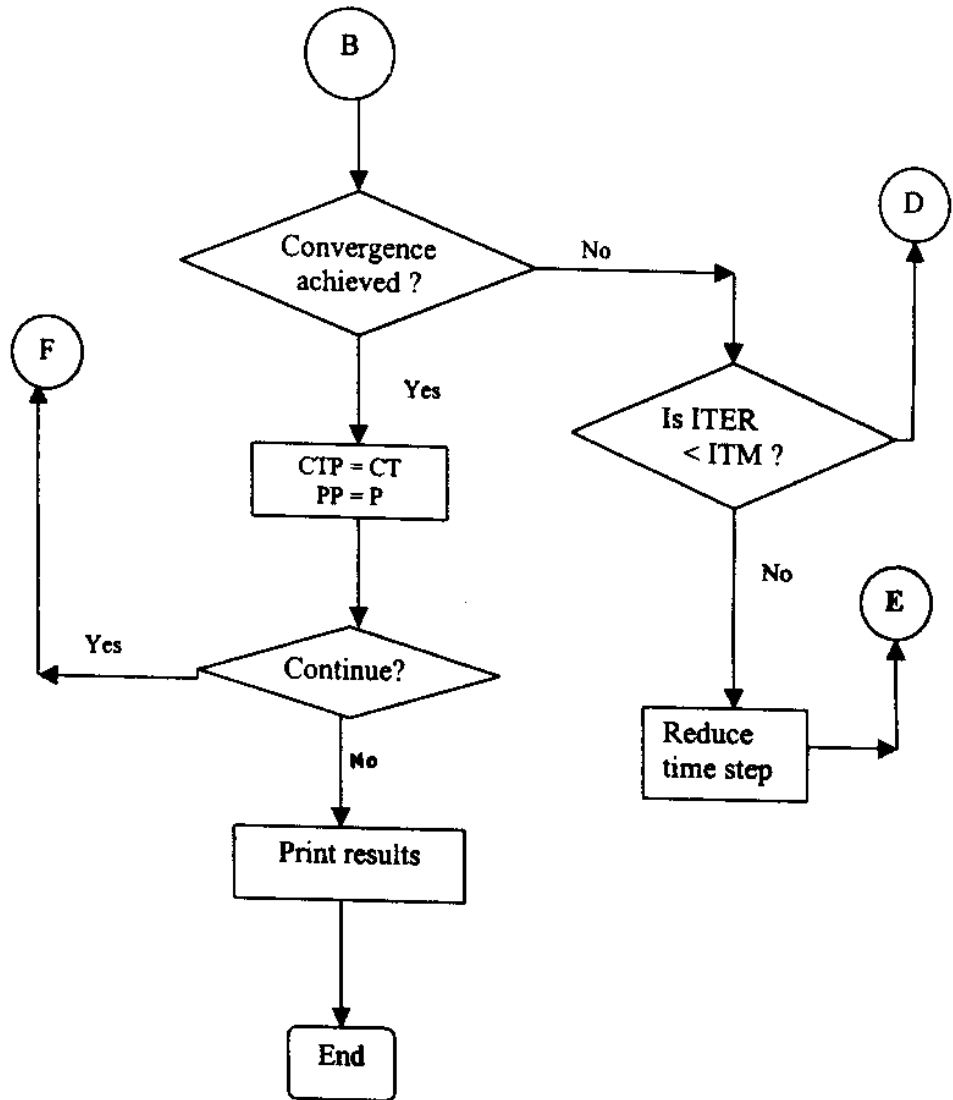
Willis, R., and Finney, B.A., (1991), 'Pacific Rim regional saltwater intrusion control', Proc. Symp. on Ground Water in the Pacific Rim Countries (H.J. Peters, ed.) Honolulu, Hawaii, ASCE, New York, pp. 57-63.

Zheng, C., (1993), 'Extension of the method of characteristics for simulation of solute transport in three dimensions', Ground Water, Vol.31, No.3, pp.456-465.

# APPENDIX - I







**General Flow Chart of Solution Strategy**

## APPENDIX - II

### Notations

$c$	: concentration of fluid
$c'$	: concentration of source (or sink) fluid
$D_0$	: coefficient of molecular diffusion [ $L^2T^{-1}$ ]
$D$	: depth of solution domain [L]
$D_{xx}, D_{xz}, D_{zx}, D_{zz}$	: coefficients of hydrodynamic dispersion [ $L^2T^{-1}$ ]
$L$	: length of solution domain [L]
$p$	: fluid pressure [ $ML^{-1}T^{-2}$ ]
$q_x$	: Darcy velocity in x-direction [ $LT^{-1}$ ]
$q_z$	: Darcy velocity in z-direction [ $LT^{-1}$ ]
$q_0$	: lateral freshwater flow from landward side of solution domain [ $LT^{-1}$ ]
$S_s$	: specific storage [ $L^{-1}$ ]
$t$	: elapsed time [T]
$v_x$	: seepage velocity in x-direction [ $LT^{-1}$ ]
$v_z$	: seepage velocity in z-direction [ $LT^{-1}$ ]
$ v $	: absolute seepage velocity [ $LT^{-1}$ ]
$W$	: source (or sink) volume flux per unit volume of the medium (+ve for inflow) [ $T^{-1}$ ]
$x$	: coordinate along the horizontal direction (+ve rightward) [L]
$z$	: coordinate along the vertical direction (+ve upward) [L]
$z_c$	: length of domain of seawater entry [L]
$z_s$	: mean sea level [L]
$\alpha_L$	: longitudinal dispersivity of porous medium [L]
$\alpha_T$	: transverse dispersivity of porous medium [L]
$\gamma$	: specific weight of fluid as a function of concentration [ $ML^{-2}T^{-2}$ ]
$\gamma_f$	: specific weight of freshwater [ $ML^{-2}T^{-2}$ ]
$\gamma_s$	: specific weight of seawater [ $ML^{-2}T^{-2}$ ]
$\kappa_x$	: intrinsic permeability in the x-direction [ $L^2$ ]
$\kappa_z$	: intrinsic permeability in the z-direction [ $L^2$ ]
$\mu$	: dynamic viscosity [ $ML^{-1}T^{-1}$ ]
$\phi$	: porosity

**Director : Dr. K.S. Ramasastry**

**Divisional Head : Sri. N.C. Ghosh, Sc. 'E'**

**Study Group : Dr. Anupma Sharma, Sc. 'B'**